AMRL-TR-69-121

VISUAL PERFORMANCE WITH SIMULATED FLARELIGHT IN ARTIFICIAL CLOUDS

SIDNEY KATZ

PAUL K. ASE

ELLIOT RAISEN

IIT Research Institute

ROBERT L. HILGENDORF, CAPTAIN, USAF

Aerospace Medical Research Laboratory

JANUARY 1970

AEROSPACE MEDICAL RESEARCH LABORATORY
AEROSPACE MEDICAL DIVISION
AIR FORCE SYSTEMS COMMAND
WRIGHT-PATTERSON AIR FORCE BASE, OHIO

DOCUMENT CONTROL DATA - R & D

(Security classification of title, body of abstract and indexing annotation must be entered when the overall report is classified)

1. ORIGINATING ACTIVITY *(Corporate author)*	2a. REPORT SECURITY CLASSIFICATION
IIT Research Institute Aerospace Medical &	Unclassified
10 West 35th Street Research Lab.,**AMD,	2b. GROUP
Chicago, Illinois 60616 AFSC,W-PAFB,OH 45433	N/A

3. REPORT TITLE

Visual Performance with Simulated Flarelight in Experimental Clouds.

4. DESCRIPTIVE NOTES *(Type of report and inclusive dates)*

Final Report, February 1969 – August 1969

5. AUTHOR(S) *(First name, middle initial, last name)*

Sidney Katz*   Elliot Raisen*

Paul K. Ase*   Robert L. Hilgendorf**

6. REPORT DATE	7a. TOTAL NO. OF PAGES	7b. NO. OF REFS
January 1970	76	17

8a. CONTRACT OR GRANT NO. In part under	9a. ORIGINATOR'S REPORT NUMBER(S)
F 33615-69-C-1386	
b. PROJECT NO.	C6173-1
7184	
c. Task No.	9b. OTHER REPORT NO(S) *(Any other numbers that may be assigned this report)*
05	
d. Work Unit No. 020	AMRL-TR-69-121

10. DISTRIBUTION STATEMENT

This document has been approved for public release and sale; its distribution is unlimited.

11. SUPPLEMENTARY NOTES	12. SPONSORING MILITARY ACTIVITY
	Aerospace Medical Research Lab.
	Aerospace Medical Div., Air Force
	Systems Command, Wright-Pat. AFB,OH

13. ABSTRACT

An environmental chamber was designed for the study of visual acuity in simulated fogs and mists. Light scattering theory was used as a basis for the design of aerosol clouds with visual attenuation comparable with that of real fogs. An experimental generator was constructed to produce the aerosols.

A study was made of the visual responses of thirty subjects under simulated night conditions with flare illumination. The variables studied included fog density, flare intensity, and a comparison between unfiltered vision and vision through a yellow haze filter. A direct correlation was observed between visual acuity and fog density levels. An interaction was also noted between visual acuity, fog concentration, and light level within the ranges studied. At increased light levels, subjects tended to show slightly less sensitivity to changes in the fog density. No evidence of improved visual performance was observed when the yellow haze filter was used.

14. KEY WORDS	LINK A		LINK B		LINK C	
	ROLE	WT	ROLE	WT	ROLE	WT
Vision						
Visibility						
Perception						
Field Illumination						
Illuminating Flares						
Reduced Visibility						
Haze, Mist, Fog						
Artificial Clouds						
Simulation						
Visual Performance						
Haze Filter						

FOREWORD

This study was performed by IIT Research Institute of Chicago, Illinois for the Aerospace Medical Research Laboratory under Air Force Contract F 33615-69-C-1386. The research was in support of project 7184, "Human Performance in Advanced Systems."

Dr. Sidney Katz was the principal investigator for IIT Research Institute. Captain R.L. Hilgendorf was technical monitor for the Aerospace Medical Research Laboratory. Engineering support in the design of the experimental facility was provided by Mr. D.K. Werle. The statistical analysis of the data was performed by Dr. F.C. Bock.

The authors wish to acknowledge the close cooperation of Lt. Col. John Simons throughout the course of the investigation and the helpful suggestions of Dr. M.W. Warrick, of the Aerospace Medical Research Laboratory. The authors also wish to thank Dr. Walter F. Grether, Dr. Warrick, Lt. Col. Simons, and Mr. G.R. Taylor of the Aerospace Medical Research Laboratory for their critiques of the draft manuscript. The report covers research performed between February 1969 and August 1969.

This technical report has been reviewed and is approved.

C.H. Kratochvil, Colonel, USAF, MC
Commander
Aerospace Medical Research
Laboratory

iii

TABLE OF CONTENTS

Page

LIST OF FIGURES

LIST OF FIGURES (continued)

LIST OF TABLES

SECTION I

INTRODUCTION

The majority of low altitude night reconnaissance and rescue missions in the Southeast Asia conflict are conducted under flarelight. In the dry season, when vehicular traffic is at its peak, the Air Force uses thousands of flares each night for field illumination. Search and rescue missions are known to have required as many as 240 flares in a single rescue mission. Contrary to popular thought about exotic sensor systems, flareships continue to be essential in low-altitude night missions.

Pilots use airborne flares for many types of operations, including:

       Navigation (staying over a target area)

       Rendezvous (marking a position)

       Reconnaissance (area search)

       Target Marking

       Target Illumination

       Ground Support Illumination

       Search and Rescue Illumination

       Disrupting Enemy Gunners

       Terminal Guidance

    and Strike Illumination

In the present report, interest is limited to the use of flares in operations involving night perception, and particularly under conditions where mist or haze degrades visibility.

1

Even in favorable weather target acquisition is considerably poorer under flarelight than under daylight conditions. (Hilgendorf, 1968). Factors potentially contributing to degradation in target acquisition include flickering shadows, diffuse terminator lines, lowered luminance levels and lack of depth cues. Under the extremely unfavorable conditions of smoke, fog, or haze, the "milk bowl" effect produced by the scattering of flare light can virtually eliminate the visual scene. In training and combat, pilots occasionally dive into the "milk bowl" (a brilliant, blinding, horizon-filling source of glare) hoping to run out of the "fire ball" in time to clear the lower cloud deck, and find and track the target.

In spite of the extensive use of flarelights and the problems associated with their use, little research has been aimed toward determining desirable placement, intensity, beam pattern spectral characteristics, etc. of flarelights. No definitive literature was found that dealt with the effects of these elements on visual acquisition.

Basic data are needed to suggest design, deployment, and training criteria for:

Flight path offset angles (minimum glare, maximum acuity)

FAC/TAC/Flareship tactics (observer positions)

Eye Filters (glare, target enhancement)

Site support tactics (battlefield illumination)

In establishing such criteria it is necessary to recognize the interactions between flarelights and ground and atmosphere

conditions. Once quantitatively understood, the environment can be used to degrade enemy performance, to enhance friendly aerial and ground observers' tasks, and to suggest new artificial light and artificial cloud applications.

This report describes a laboratory procedure for studying the effects of fog or mist on visual acuity under conditions of night illumination. In a real situation, the distances may be thousands of yards,mist or fog particles of varying concentrations and compositions may be present and there may be a miscellany of natural and man-made effects including the condition of the terrain, the night illumination in the environment, etc. The argument for simulation is the ability to duplicate, control, and evaluate a particular set of conditions rather than depend on its fortuitous occurrence and availability in the natural environment. In addition to convenience, substantial savings in cost and effort can be expected from a properly designed simulation experiment.

SECTION II

ATTENUATION OF VISION IN THE ATMOSPHERE

MECHANISM OF ATTENUATION

Middleton (1952) has discussed in considerable detail the
problems related to vision through the atmosphere.

An object is observed in relation to its visual background.
In general, one's ability to see an object depends on its size,
its luminance, the luminance of the background, the contrasting
chromaticity (color), the presence of distracting objects in the
field of view.

The visual size of an object is observed as a solid angle
with the eye at the apex and the object as the base of a right
cone. Traditionally, it is measured as the plane angle with
the eye at the apex and the diameter of the object as the base
of an isosceles triangle. A size threshold exists which is
fixed for a given luminance-contrast threshold and background
luminance level (Blackwell, 1946).

The "Brightness contrast," C, is generally defined in terms
of an object's luminance, B, and the luminance of its background,
B',

$$C = \frac{B-B'}{B'}$$

If the object is darker than its background, the contrast is
negative and if it is brighter, the contrast is positive.

Under conditions of uniform haze density, brightness
contrast can be analyzed mathematically. The alteration of

4

luminance contrast by the atmosphere under daylight conditions is discussed by Middleton.

An object whose inherent luminance is B_o, and background luminance is B_o', becomes less distinct as the viewing distance increases. At a great distance, the object may become indistinguishable from the background. Inherent contrast is defined as

$$C_o = \frac{B_o - B_o'}{B_o'}$$

At a distance, R, the apparent contrast, C_R, is

$$C_R = \frac{B_R - B_R'}{B_R'}$$

where B_R and B_R' are the apparent luminances of the object and the background, respectively at the distance R.

Apparent contrast is related to inherent contrast by:

$$C_R = C_o \ (B_o'/B_R') \, e^{-\sigma R}$$

where $e^{-\sigma R}$ is the attenuation of the light by the atmospheric haze. R is the distance from the object to the eye. It is assumed that the haze is made up of particles, which are transparent in the visible region of the spectrum and σ is the extinction coefficient in the given direction for these particles. The particles in the atmosphere are assumed to be homogeneously distributed, both laterally and vertically.

The last equation relates the apparent contrast, C_R to the inherent contrast, C_o, the ratio of the background luminances, (B_o'/B_R'), and the light transmittance, $e^{-\sigma R}$. Thus, if one

5

could determine the σ corresponding to the haze level, it would be possible to predict apparent contrast at distance, R.

Apparent contrast has been expressed in a slightly different form by Sawyer (1950) as

$$C_R = \frac{(B_o - B_o')\ e^{-\sigma R}}{B_o' e^{-\sigma R} + G}$$

where the terms have the same meaning as before. G is a glare factor term. $(B_o - B_o')$ is the difference between the inherent luminance of an object and its background. Thus, in the numerator, the inherent luminance difference is reduced by $c^{-\sigma R}$, to give the apparent luminance difference. The denominator combines the transmitted light with the background scattered glare to give the apparent background luminance.

Here again, given the haze level and assuming it can be quantified, it would be possible to calculate the apparent contrast.

The eye will distinguish contrast differences down to a lower limit called the threshold contrast, C_T. Objects of a given size will be obscured if

$$C_T > \left| \frac{B_R - B_R'}{B_R'} \right|$$

Blackwell, (1946) relates the threshold for brightness difference, $(B_R - B_R')$ to B_R' for a wide range of background brightness.

In Figure 1 the log of the brightness contrast threshold, log C_T, is plotted against the log of the background brightness, log B', for several visual angles. The contrast threshold remains low and constant at high background brightness levels and then increases rapidly at lower levels. At any given background level, the contrast threshold decreases with the visual angle of the target. The knees in the curves occur where the visual process

6
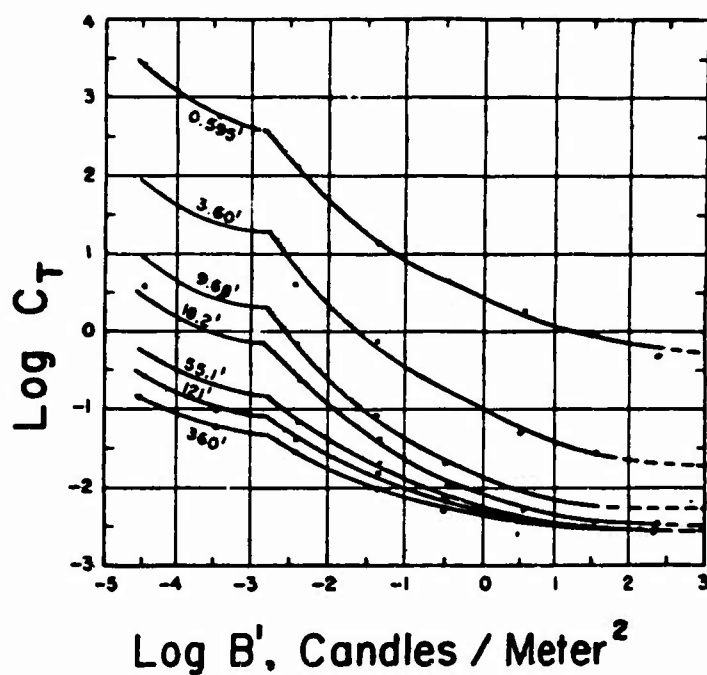
Figure 1.   BRIGHTNESS - CONTRAST   THRESHOLD C_T
AGAINST BACKGROUND BRIGHTNESS B'
FOR VISUAL ANGLES FROM 0.595' TO 360'
(Blackwell, 1946)

7

switches from cone to rod activity. The switch occurs at a fixed, low background level and is apparently independent of the contrast threshold over a wide range of visual angles.

In daylight the light source is the sun and all particles in the terrestrial atmosphere may be considered equidistant from the source. Furthermore, the scattering angle can also be considered to be the same for all of the particles in a given obeserver-target geometry.

In the context of flarelights at night, the source is close to both the target and the observer, and thus we have essentially a localized illumination against a dark background. In a typical combat or rescue situation, the viewer is airborne at a moderate altitude, i.e., 1000 to 5000 ft. Naval Mark 24 flares are commonly used; a new flare, the Naval "Briteye" is under development. Both flares have magnesium-sodium nitrate compositions and are rated at 2,000,000 and 5,000,000 candle power, respectively.

Vision is attenuated in a natural fog by light scattering. Scattering is a function of the wavelength of the light, scattering angle, the nature of the material, and concentration of the particles. Although the exact mechanism of light scattering is complex, the effect is to decrease the radiation from the object to the eye, and to increase the brightness of the background against which the object is observed. Light scattering does not appear to decrease visual acuity by simply degrading optical resolution (Middleton, 1952, p. 78). In the present paper the discussion is limited to spherical particles and to nonabsorbing scatterers. This is a valid restriction since natural fogs are arrays of spherical water particles which are essentially transparent in the visible

8

wavelength region.

The objective of the work reported here is the observation, under laboratory conditions, of the effects of a simulated foggy atmosphere on visual acuity.

Because of their topical interest as visual aids in foggy atmospheres, yellow filters were included in the study. Stuart (1934) states that white light seen through a fog appears yellow and recommended a headlight filter with a sharp cutoff below the yellow for use in night fog driving. Miller, Martin, and Dohrn (1963) describe the particular yellow filters used in the present tests. The filter which is commercially available* transmits almost totally in the visual range from 520 mμ to the longwave limit of normal visibility and cuts out all the shortwave end of the spectrum below 490 mμ. A representative transmission curve of these filters is shown in Figure 2.

OPTICAL PROPERTIES OF SMALL PARTICLES

The concept underlying the design of a fog simulation facility is based on the mechanism of light attenuation by suspended small particles. This mechanism allows the duplication, in a small volume, of the attenuation occurring in a much larger space.

The interaction between a particle and electromagnetic radiation, including visible light, leads to a redistribution of the radiation. That part of the light which is not absorbed by the particle is said to be "scattered". In the present discussion we shall assume that <u>all</u> energy incident on the

---

*Bausch and Lomb Kalichrome C yellow filter.

9
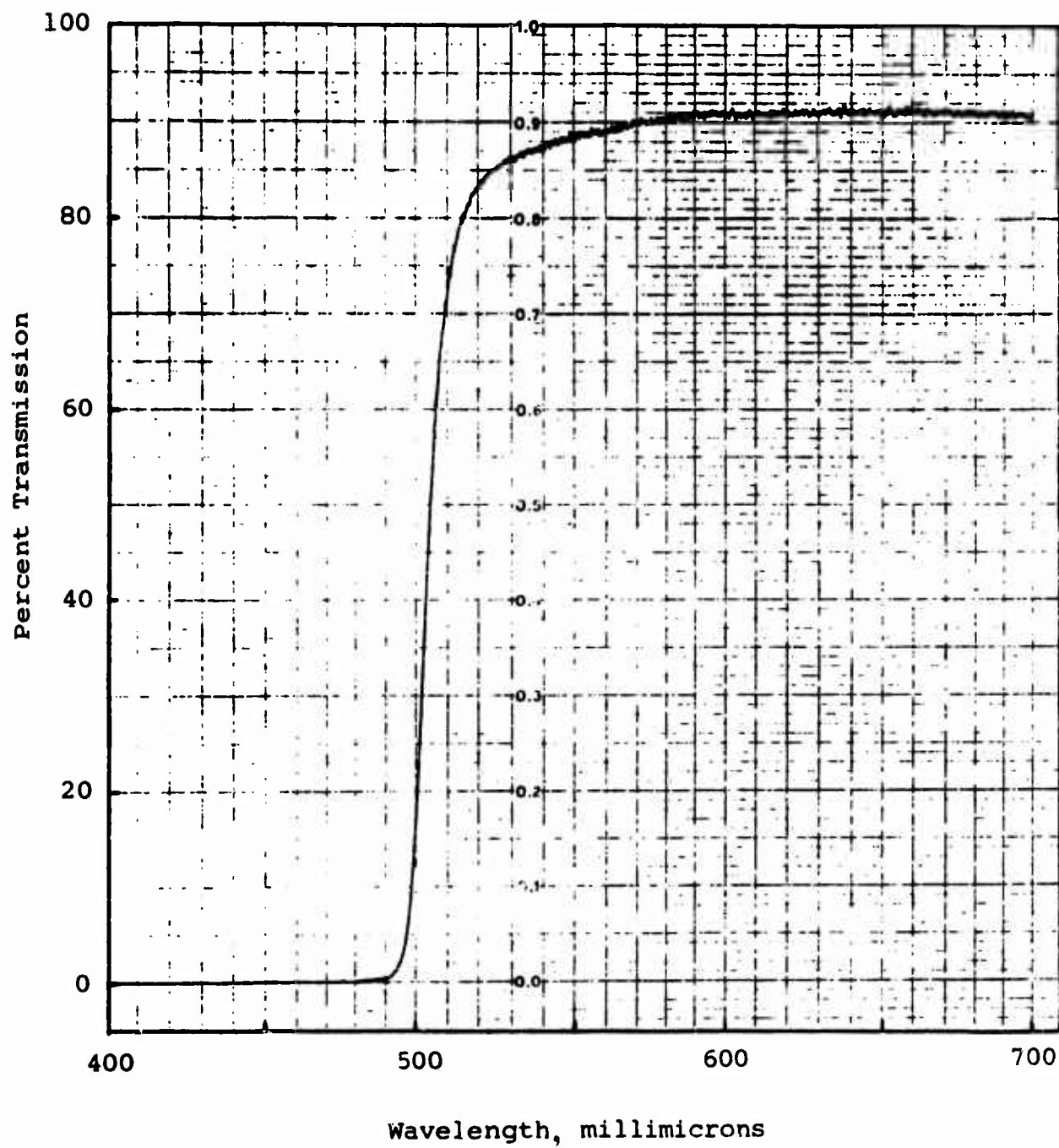
Figure 2.   Transmission Curve for Yellow Filter

particle undergoes scattering.

It was shown by Mie (1908) that light scattering by small particles can be treated by the appropriate application of electromagnetic theory; however, the detailed mathematics of his analysis is very complex. The solutions for the total and radial distribution of the light scattered by a transparent sphere show that the scatter is fully described as a function of only three parameters -- the particle size, the refractive index of the particle referred to the surrounding medium, and the wavelength of the light.

Rayleigh (1899) studied the scattering properties of very small particles and, prior to Mie's work, noted that the total scatter of a small sphere of radius r, illuminated by light of unit intensity (unit energy per unit area) of wavelength λ is,

$$S = 24\pi^3 \left(\frac{m^2 - 1}{m^2 + 2}\right)^2 \frac{V^2}{\lambda^4} \tag{1}$$

V is the volume of the particle and m is its refractive index. S is thus the effective scattering area of a particle.

This relation holds for particles for which $r \leq 0.1 \lambda$. From Equation 1 it is seen that scattering intensity is a sixth power function of the radius and an inverse fourth power function of the wavelength of the source.

The intensity, I_θ, of the scattered light at a given angle θ at a distance R when the incident light is unpolarized is

$$I_\theta = \frac{9\pi^2}{2R^2} \left(\frac{m^2 - 1}{m^2 + 2}\right)^2 \frac{V^2}{\lambda^4} \left(1 + \cos^2 \theta\right) \tag{2}$$

11

R is the distance from the particle to the point of observation and θ is the angle between the incident light source and the direction of the scattered light. Conventionally, the reverse of the direction of propagation of the incident light is 0° and the forward direction is 180°.

Even though the incident light is unpolarized the scattered light consists of two plane-polarized components, with the planes mutually at right angles. If we identify these components by their intensities, i_1 and i_2, then i_1 is the vertically polarized component, and i_2 is the horizontal component. The $\cos^2 \theta$ term in Equation 2 governs the value of i_2 and the factor of unity governs i_1 which is therefore constant in intensity at all angles.

For the general case of Mie scattering, the angular intensity corresponding to Equation 2 is

$$I_\theta = \frac{\lambda^2}{8 \, \pi^2 \, R^2} \; (i_1 + i_2) \tag{3}$$

and the total scatter, S, is given by the sum of the series,

$$S = \frac{\lambda^2}{2\pi} \sum_{n=1}^{\infty} (2n+1) \; (|a_n|^2 + |b_n|^2) \tag{4}$$

The terms i_1 and i_2 in Equation 3, and a_n and b_n in Equation 4 are defined in Appendix I. Two useful additional terms are the total scattering coefficient, K, equal to $S/\pi \, r^2$, and a scattering parameter, α, equal to $2\pi r/\lambda$, i.e., the ratio of the particle circumference to the wavelength.

12

Scattering functions have been computed for a number of conditions. Figure 3 shows how the total scattering coefficient K varies with α for a single particle with a refractive index (m) of 1.33, i.e., water. In Figure 4 the total scattering area per unit weight is plotted for spherical water droplets, against the radius for a selected value of λ (.555 mμ). The rapid decrease in scattering efficiency of Rayleigh scatterers as the particle size is reduced, predicted by Equation 1, is noted in Figure 4.

The radial distributions of the intensity of the radiation scattered by water droplets of varying α's are shown in Figure 5. The figure illustrates the characteristic forward and backward symmetry of the scattered intensity when α is small and the strong forward scattering intensity, and the numerous additional scattering "lobes" which appear as α increases.

It can be seen in Figure 5 that the number of intensity maxima of the i_1 component of the radial distribution increases with increasing α. The visual phenomenon which is called the "higher order Tyndall effect" appears as a succession of color maxima and minima when a cell containing a nearly monodisperse aerosol is illuminated by a narrow parallel beam of light and is viewed at different angles. The red bands are the most conspicuous, and a rapid and moderately accurate determination of the radii of the aerosol particles can be made by using white light and either counting the number of red bands and multiplying by 0.1 or noting the angle at which the first red band

13
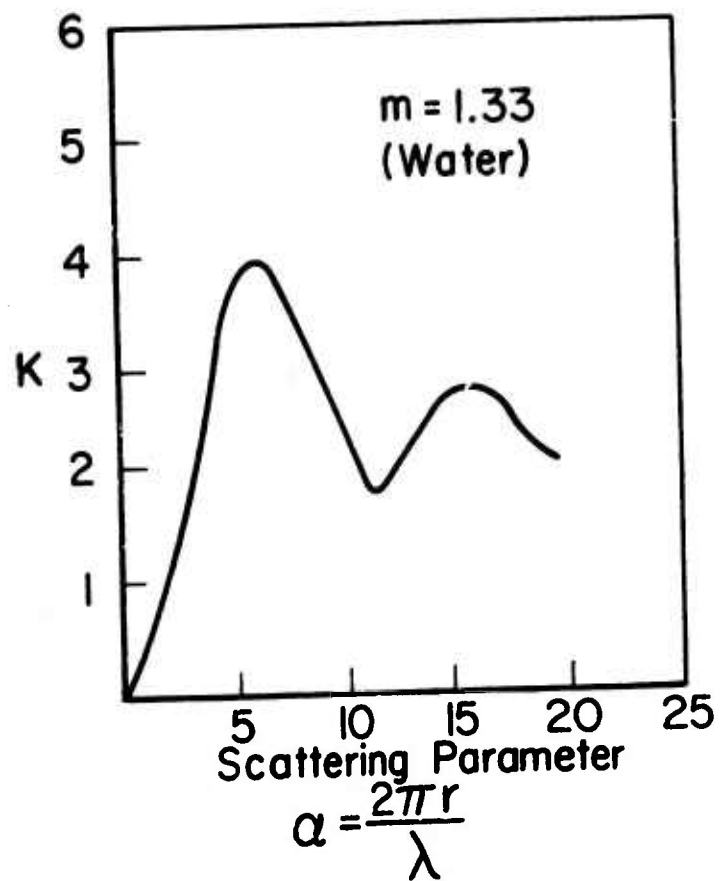
Figure 3. SCATTERING COEFFICIENT K
OF A SPHERICAL PARTICLE

14
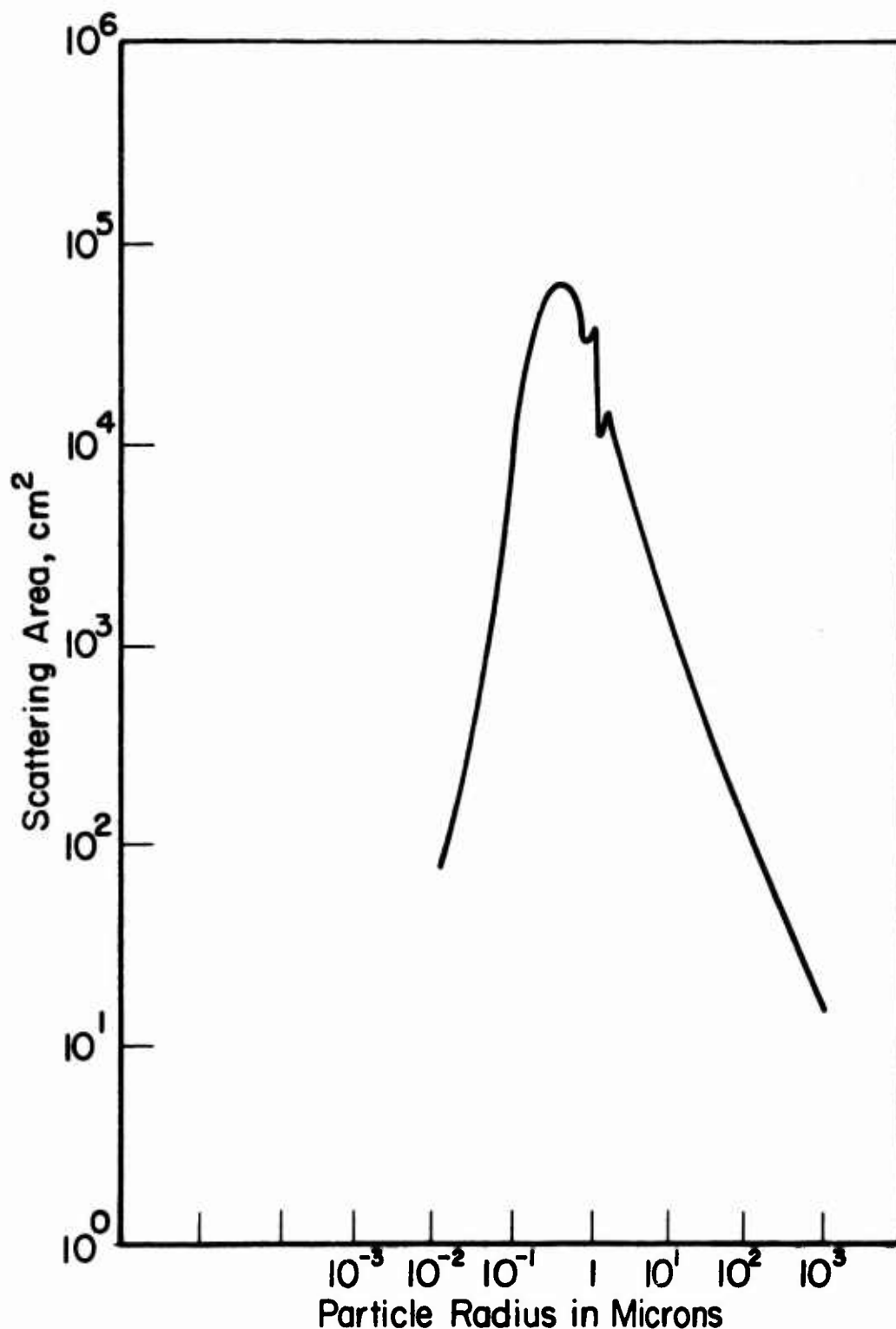
Figure 4. TOTAL SCATTERING AREA OF AN AEROSOL
CLOUD OF SPHERICAL PARTICLES OF ONE
GRAM WEIGHT, PARTICLE DENSITY OF I,
AND REFRACTIVE INDEX OF 1.33 AT 0.55
MICRONS WAVELENGTH

15
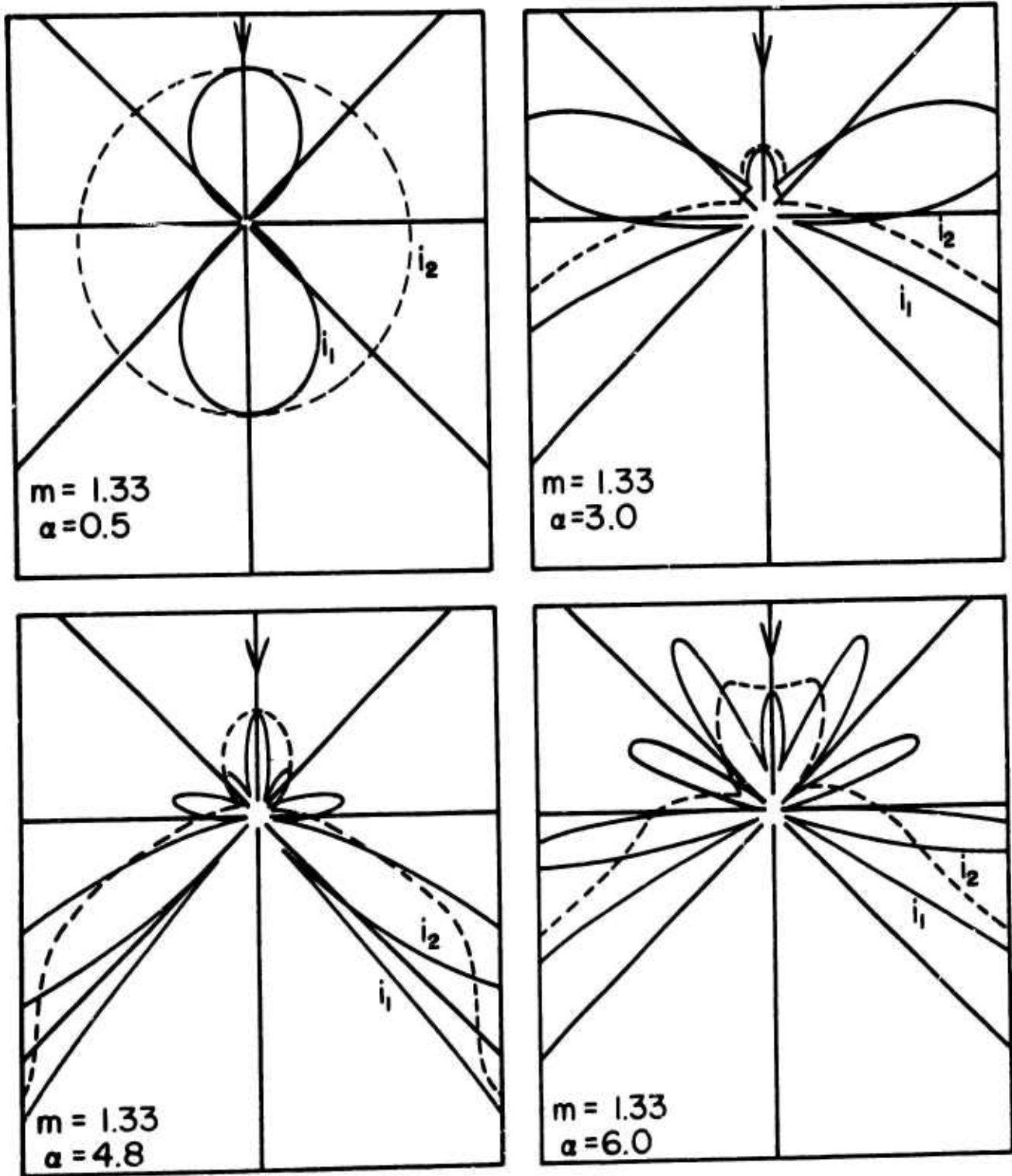
Figure 5. Radial Distribution of Intensity of Light Scattered by Spherical Particles. The Particle is at the Intersection of the Axes and the Arrows Indicate the Direction of the Incident Light.

16

appears*. This method is, however, not recommended for materials whose refractive index is greater than 2, or for particles much larger than 1.5 microns diameter.

The equation for the transmission of light through a cloud of particles is given by the relation

$$t = I/I_0 = e^{-\pi r^2 Knl} \tag{5}$$

where t, the transmission, is the ratio of I and I_o, the emergent and incident intensities, respectively, of a light beam passing through the cloud. K is the scattering coefficient, n is the particle concentration per unit volume, r is the particle radius, and l is the length of the path through the beam.

In the present work equivalent fogs are designed by the application of Equation 5. "Equivalent" fogs are defined as fogs of equal light transmission under conditions in which the path length, l, is defined and r, n, and the refractive index, and hence K, can be adjusted. Considerations of material availability and stability, ease of production, etc., all influence the selection of equivalent fogs.

LABORATORY ANALOGUES

Green and Lane (1964) distinguish between mists and fogs, noting that "a light mist" consists of water droplets ranging from 10 to 50 microns in diameter. Middleton (1952) avoids use of the term "mist" and instead differentiates a "fog", where the particle diameters are greater than about 4 microns, from "haze",

---

*Appendix III.

17

in which the particles are below that size. Natural fogs, mists, and clouds vary greatly in both particle size distribution and particle concentration. Kneusel (1935) reported a valley fog with particles about 4.4 microns median diameter and a mountain fog or cloud with particles of 14 microns maximum diameter. These figures are probably low. Houghton (1940) gives corresponding diameters of 22 and 46 microns for a coastal and a mountain fog. Bricard (1939) gives 20, 16, 10, and 8 microns for the particle diameters in nimbostratus, stratocumulus, cumulus, and stratus clouds, respectively. Houghton and Radford (1938) report droplet concentrations of 5 to 50 x 10^3 droplets/ml for clouds and 0.1 to 1 x 10^3 droplets/ml for fogs. Sinclair (1950) states that a dense natural fog of 20 microns median diameter contains about 10^3 particles per ml.

One may consider a 2000-ft thick, water droplet mist, composed of 20 micron diameter particles. Let it be assumed that a parallel beam is attenuated to 10% of its incident intensity by this mist. Assigning to K, the scattering coefficient, a value of 2, Equation 5 shows the aerosol concentration, n, to be 6 particles/ml. For particles which are large relative to the wavelength, the scattering coefficient is insensitive to wavelength, as shown in Figure 3, and the wavelength need not be specified.

To design a fog of equivalent attenuation in a small volume, it is possible to increase the concentration of the scatterer, the scattering efficiency, or both. Assuming the reduced volume to involve a light path of 9-ft, then a fog of 20 micron-diameter

18

particles equivalent to the 2000-ft path and 6 particles/ml, would contain about 1400 particles/ml, corresponding to an aerosol weight of 5.8 x 10^{-6} g/ml. Such a dense aerosol would be difficult to stabilize in an experimental system. A more feasible alternative is to select particle parameters to maximize scattering efficiency.

The scattering efficiency for water and its dependence on λ and particle size were shown in Figure 3. If we design a cloud for 0.550 microns wavelength, the scattering efficiency coefficient has its maximum of 3.9 when the particle diameter is 1.05 microns. Again assuming a light path of 9-ft, a concentration of 2.6 x 10^5 particles/ml, weighing 3.15 x 10^{-7} g/ml, will produce an attenuation equal to that in the reference 2000-ft path.

It is also possible to replace the water aerosol with particles having a higher refractive index which would be somewhat more efficient scatterers. For example, stearic acid spheres of 0.88 micron diameter have a scattering coefficient of 4.2, and a stearic acid cloud, equivalent to the 2000-ft mist path, would contain 3.3 x 10^5 particles/ml weighing 1.2 x 10^{-7} g/ml.

Although it is possible to generate aerosols of even greater scattering efficiency, stearic acid was selected because its optical properties have been extensively described and because it has been used in generating precisely sized, stable aerosols.

DISPERSAL AND STABILITY OF SMALL PARTICLES

The LaMer generator (Sinclair and LaMer, 1949) is used for the production of monodisperse liquid aerosols. In its operation

19

a stream of hot air passing over a heated liquid, collects the
vapor above the liquid and transports it through a chimney.
Here it is cooled slowly under carefully controlled conditions
and the aerosol precipitates out in a narrow range of particle
sizes. Stearic acid is a solid at ambient temperature but with
a melting point of 70°C, and it can therefore be used to form
an aerosol of liquid particles. These particles supercool
before solidifying and retain a nearly spherical shape as they
solidify.

An aerosol cloud is inherently unstable. This condition
arises because of a number of cooperating factors, several of
which are considered here. The vapor pressure of a liquid
which, in the case of macroscopic quantities tends to be simply
temperature dependent, also becomes size dependent when the
particle size is reduced greatly. Thus, a very small particle
will have a higher vapor pressure than a somewhat larger
particle and consequently large particles tend to grow and
smaller particles disappear.

Small particles disappear through collision which may be
induced by convection currents, settling, and Brownian movement.
Brownian movement is an erratic motion exhibited by very small
particles in gaseous or liquid suspension. Particles are under
constant molecular bombardment. When the cross section is small,
the probability that this action is symmetrical is low. The
differential forces thus generated impart a random motion to
the particles. This motion may be considerable in the submicron
particle size range. Above a diameter of about a micron,

the effect is slight.

Settling is usually the most serious cause of instability in an aerosol. Stokes law defines the settling velocity of a small particle (less than 100 microns) by the relation

$$u = Gd^2 \frac{\rho - \rho_0}{18\eta} \tag{6}$$

where ρ and ρ_0 are the densities of the particle and the medium, respectively, d is the particle diameter, η is the viscosity of the medium, and G is the gravitational constant. In a poly-disperse aerosol, differential settling rates cause the faster falling, larger particles to sweep up the smaller, more buoyant particles, thus increasing the aerosol breakdown.

Table 1 lists the Stokes law settling-rates of several sizes of spherical particles in air. In the cases of the two smallest particles listed, collision induced by Brownian movement contributes more significantly to the particle instability than gravity.

Table 1

Settling rates in air at 21°C
of small spherical particles of unit density

Particle Diameter, microns	Settling Rate, microns/sec
0.1	0.86
0.25	3.1
0.5	10.0
1.0	34.3
2.5	200.0
5.0	775.0
10.0	3050.0

It is evident that an experimental aerosol which must be stable for an appreciable time should consist of small, uniform

21

particles of low density and, of course be in a size range consistent with the optical requirements of the experiment. It should preferably be a solid with a low vapor pressure. For good definition of its optical properties, it should consist of spherical particles. Since a stearic acid aerosol can be made to embody these properties it is well suited to the present application.

RECAPITULATION OF LABORATORY ANALOGUE CONCEPT

In the previous section, the composition of natural fog was described and its elements examined. Light scattering theory was reviewed insofar as it appeared to be related to problems of designing a laboratory model of the fog, and a number of scaling factors were noted.

The underlying assumption in the design of the laboratory model is that analogue conditions are maintained when the light attenuation and scattering characteristics of real clouds are preserved. Attenuation of the target is caused by the reduction of its optical signal by the scatter from intervening aerosol particles and by the loss of contrast due to the scatter of light from all other particles in the visual background. It is assumed that in both cases the scatter can be related to the number of particles and their scattering cross sections and, further, that this condition can be duplicated with an "analogue" aerosol in which the number and size of particles can be varied, provided that the total scatter is preserved. Carrying this concept a step further, it is reasoned that, if these conditions are

22

maintained, the analogue aerosol material may be different from the real aerosol. The dimensions of the analogue aerosol may be quite different from those of the real aerosol, provided that the optical relationships are preserved.

As a first approximation, a very long optical path in an aerosol may be compressed and, provided the shortened light path does not increase the concentration of the particles to the point where they interact as light scatterers, the scattering properties should not be disturbed. However, problems of aerosol stability arise when many large particles exist in a small volume.

The obvious answer is an aerosol composed of a larger number of smaller particles, specifically replacing the water aerosol with a nonaqueous low vapor pressure material having light scattering efficiency. Thus, a lesser weight of material can be used; the particle spacing in relation to particle size can be increased; settling rates can be diminished; and there will be less tendency for particles to agglomerate on collision.

The ability to control these variables lends flexibility to the whole analogue concept.

23

SECTION III

EXPERIMENTAL STUDIES

The experimental studies consisted of a series of visual acuity tests conducted in an aerosol chamber in which light level and aerosol concentration were controlled. All subjects were tested with and without yellow optical filters.

The experimental conditions are described in detail below:

TEST SUBJECTS

The test subjects were thirty male employees of IIT Research Institute between the ages of 20 and 35. All subjects passed the Titmus eye test with natural or corrected vision of 20/20 or better. The Ishihara Pseudo-Isochromatic Plates were used to detect the presence of color deficiency. Following the conclusion of the experiments, one subject was found to have a slight color-blind condition. His test results are well within the range for his group and so his data are included in the results.

EXPERIMENTAL SYSTEM

(1) TEST CHART

The test chart was a modified Landolt C chart (Graham, Bartlett, Brown, et al, 1966). A standard Landolt C is a black C on a white background. The C is circular with the thickness of the C outline equal to 20% of the circle diameter and also equal to the gap in the circle. Thus the gap forms a square.

24

The C's are oriented with the gap facing any of four directions, up, down, left, or right. The standard chart consists of several rows of C's of increasing sizes, with all C's in a row the same size. A test consists of identifying the orientation of the gap.

In the present work, the chart color was reversed - white C's on a black background - and complete circles were added. The chart consisted of 70 Landolt C and modified Landolt C elements in rows of five elements in a continuously decreasing series. Any two consecutive pairs of C's had their diameters in the following ratio:

$$\frac{D_n}{D_{n+1}} = 1.0592$$

where D_n and D_{n+1} are the outside diameters of two consecutive C's. The diameter of the largest C was 10 cm and the smallest was 0.1883 cm. A portion of a chart is illustrated in Figure 6 and the details of its construction are given in Appendix II.

The reflectance spectra of the white Landolt C letter and the black chart background were measured with a General Electric reflectance spectrometer. The spectra are shown in Figure 7.
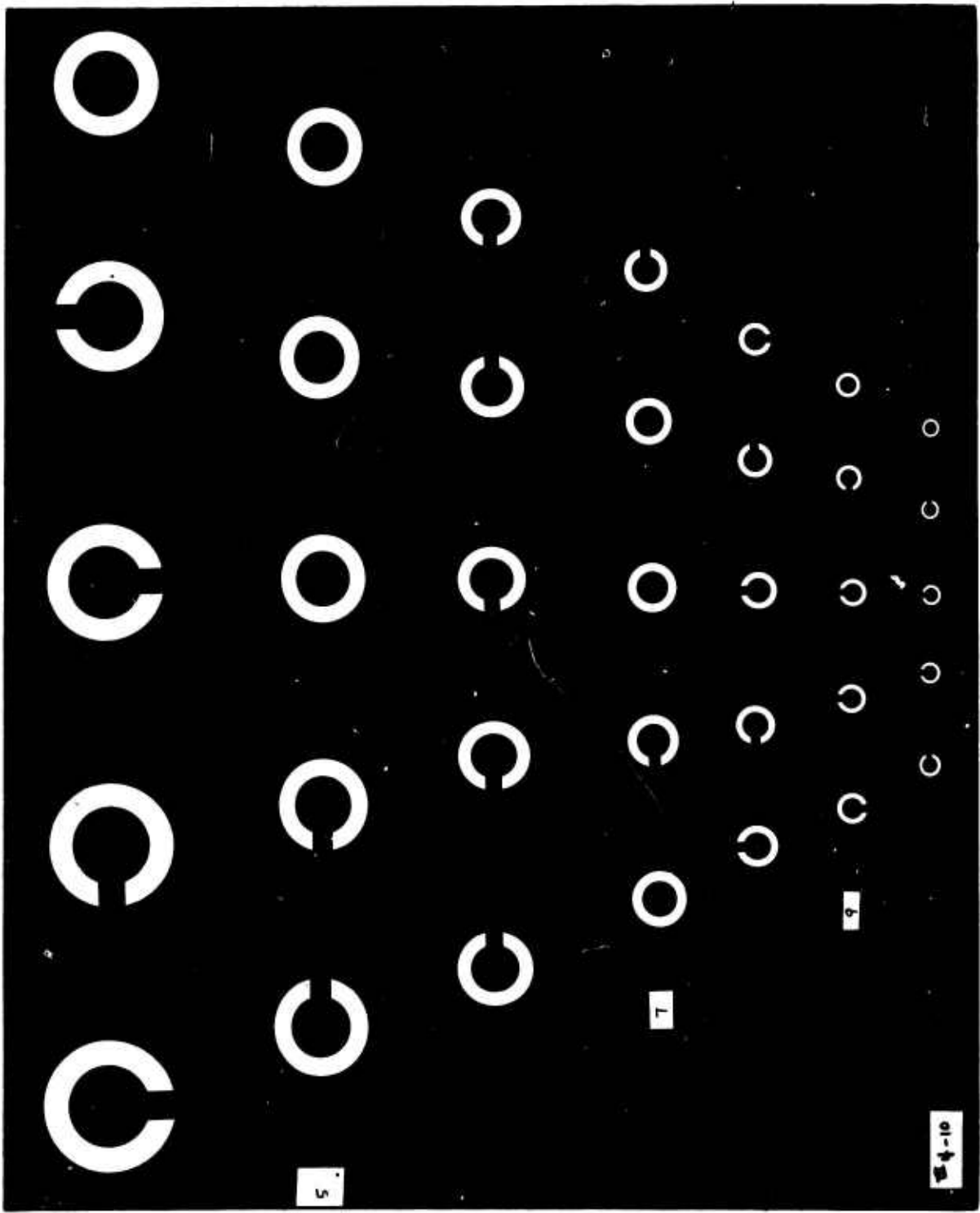
Figure 6. Test Chart
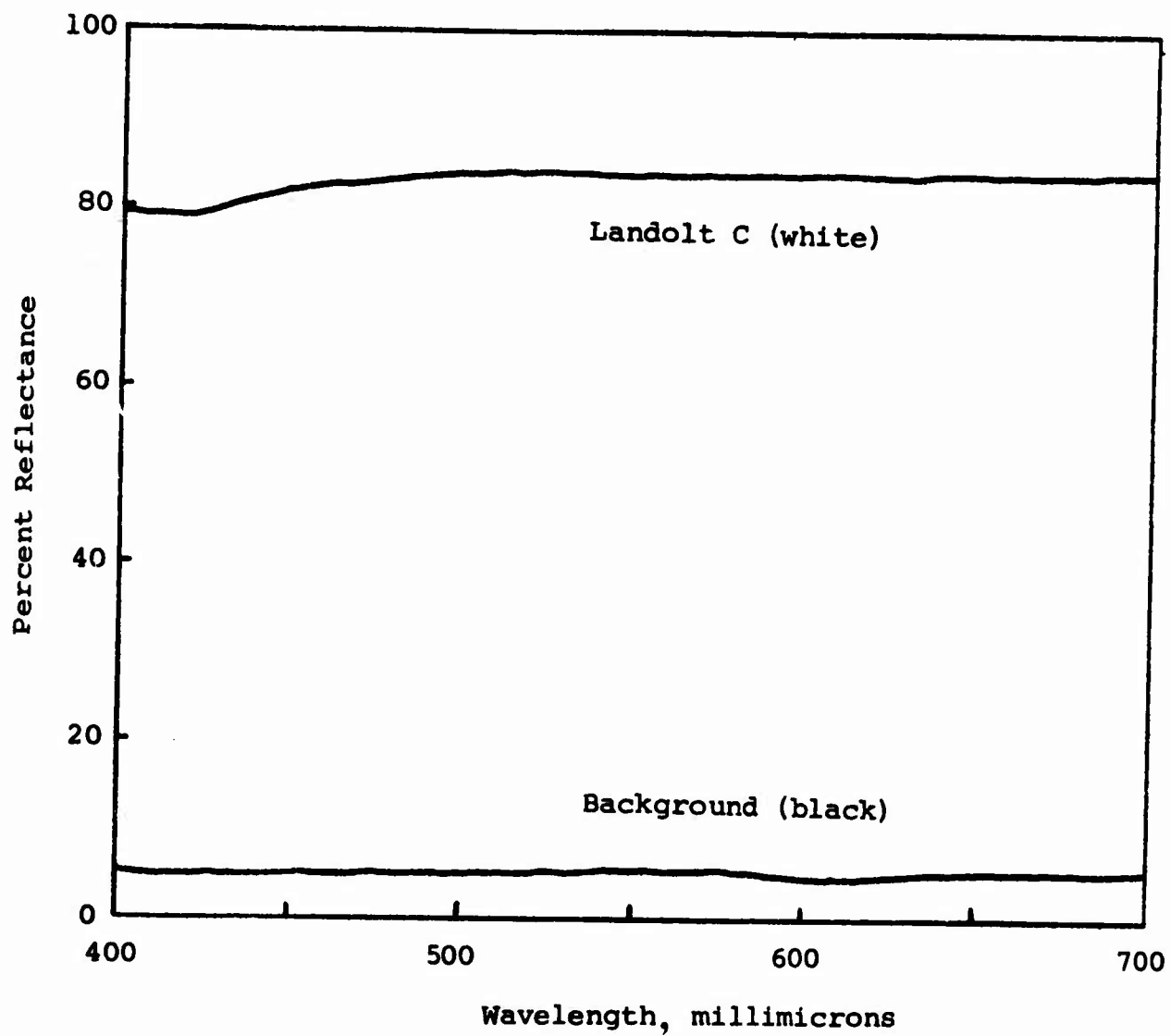
Figure 7. SPECTRAL REFLECTANCE OF CHARTS

EXPERIMENTAL FACILITY

The experimental facility was designed as a scale simulation of a night operation under flare illumination in a light mist. The simulation chamber was a darkroom with walls, floor, and ceiling covered with a black, plastic sheet coated with flat black latex paint. The Landolt C chart was near floor level and a light source was suspended 9 ft above the center of the chart. Two million and five million candlepower flares suspended at 2000 ft were adopted as reference sources. These flares would yield 0.5 and 1.25 ft candles of ground level illumination, respectively, directly below the flares. The corresponding chamber source illumination at 9 ft above target level would be 40 and 100 candlepower.

Representative experimental conditions used in the chamber were:

Light source height	9 ft
Source luminous intensity	40 and 100 candlepower
Aerosol	stearic acid
Aerosol particle diameter*	0.68 microns
Aerosol concentration, particles/ml*	2.5×10^5 and 5.0×10^5
Aerosol refractive index	1.433

Basing the calculations on a monodisperse mist of 20 micron particles, and a wavelength of 550 mμ the corresponding

---

*Experimentally determined.

28

"real" conditions (Figure 8) are:

Flare height	2000 ft.
Flare intensity	2.0×10^6 and 5.0×10^6 candlepower
Flare color temperature	2400 to 2600°K
Observer height	2000 ft
Observer viewing angle from horizon	-45°
Mist particle diameter	20 μ
Mist concentration, particles/ml	1.5 and 3.0
Refractive index of water	1.333

A General Electric No. W 1156 tungsten filament lamp operating at either 12.6 or 16.8 volts was used for the chamber light source. At these voltages, it gives the required light levels of 40 and 100 candlepower and filament color temperatures of 2536 and 2783°K, respectively.

Figure 9 is a drawing of the aerosol chamber and Figure 10 shows the chamber in plan. Two walls of the chamber coincide with the walls of the room. The third wall forms, in plan, a 145° circular arc. The axis of the arc is a vertical line along which the light source is suspended. Thus all positions along the projected arc are equidistant from the light. Observers can be placed at either of two rows of windows, one at normal eye level, and one at 9 ft above the floor. In the present series of observations, only the upper level was used.
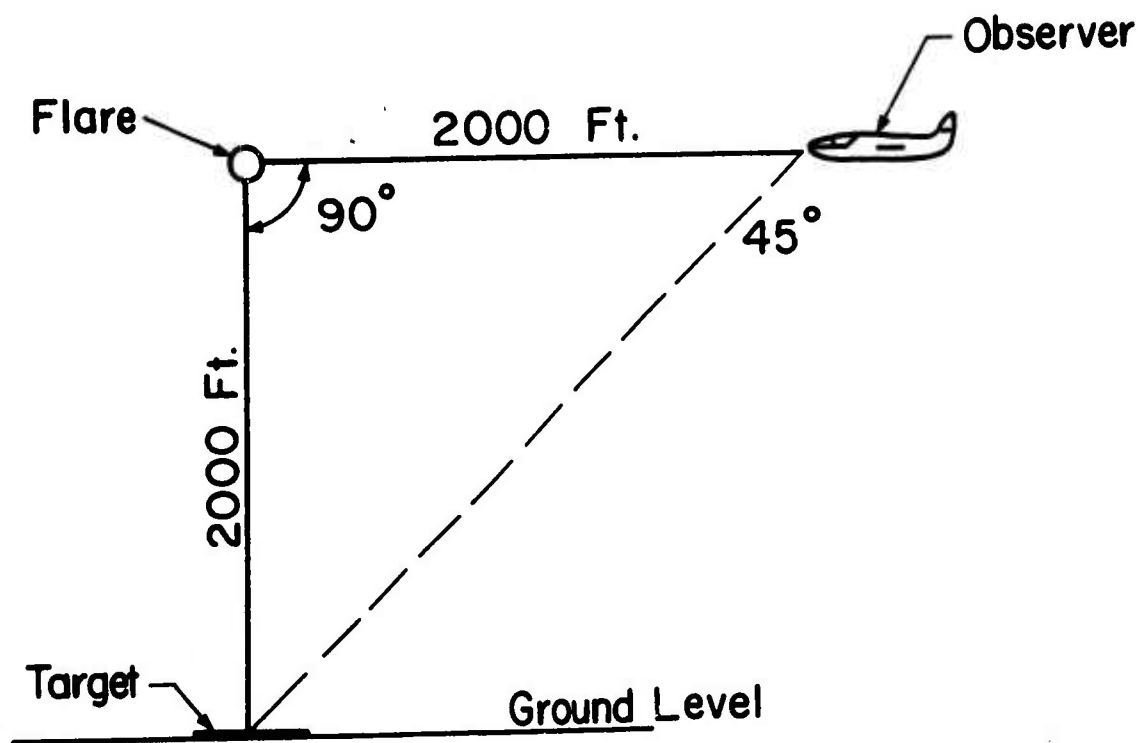
Figure 8.   FIELD SYSTEM CONFIGURATION
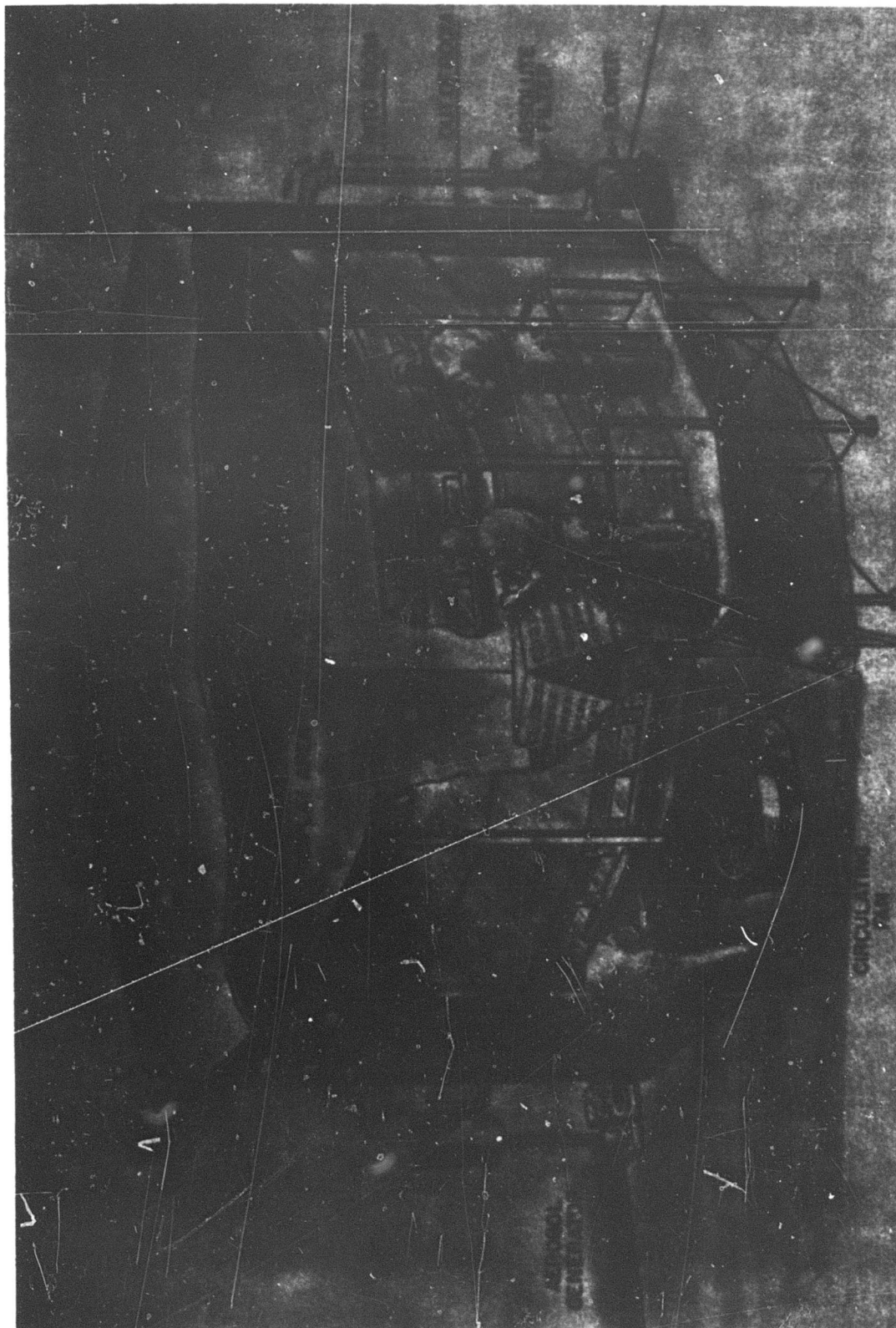
Figure 9. Aerosol Laboratory
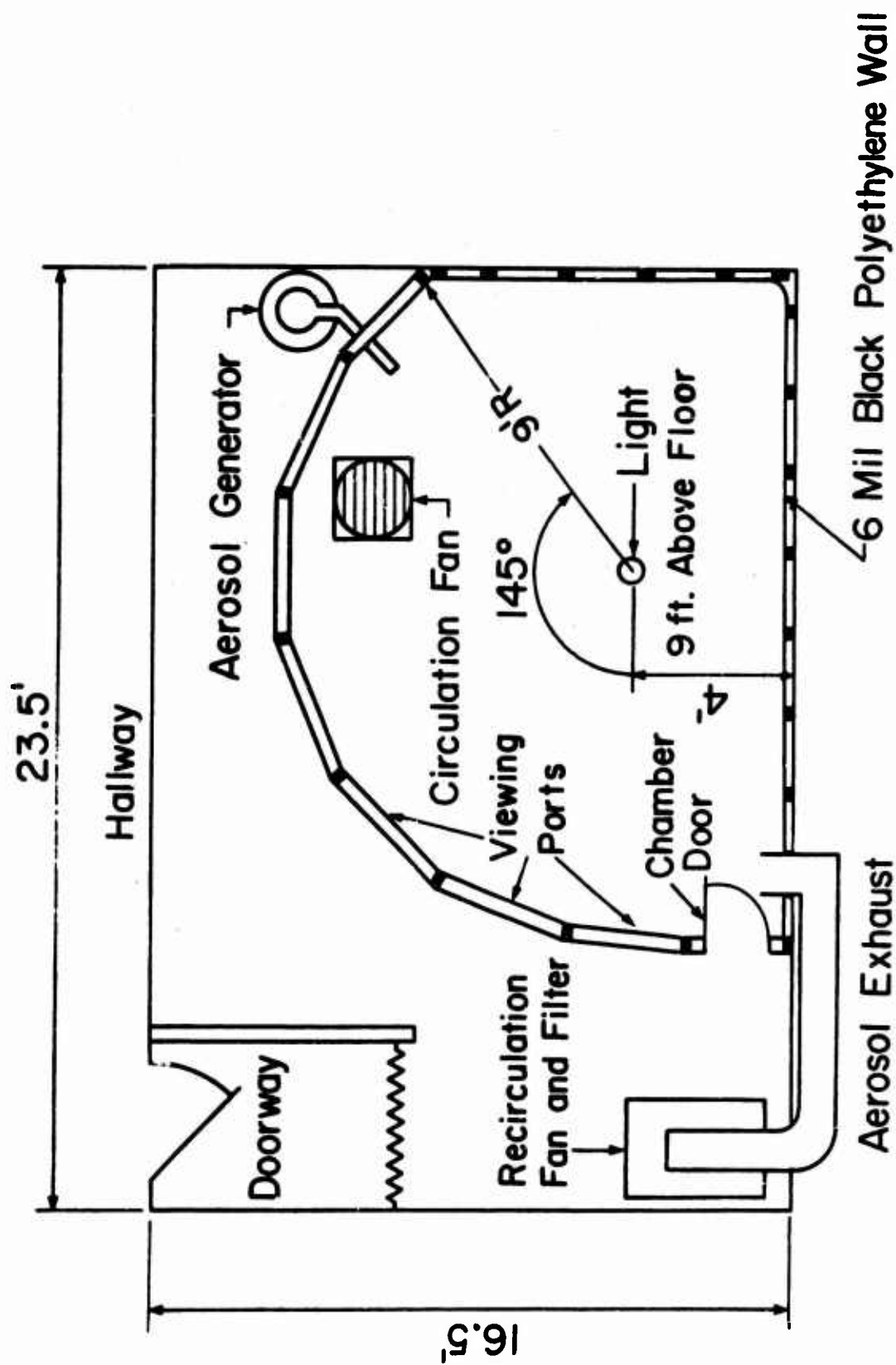
Figure 10. FLOOR PLAN OF AEROSOL CHAMBER LABORATORY

32

The aerosol generator, a modified LaMer generator is shown in Figure 11 and 12, and also at the left in Figure 9. Operation of the generator was described on page 19.

The aerosol inlet to the chamber, the aerosol circulating fan and the aerosol removal system are shown in Figure 9. The aerosol is removed by circulating the chamber air through an absolute filter which retains the particulate matter. In addition a sampler consisting of a filter, and a calibrated pump samples the aerosol by collecting the aerosol from a measured volume of air. The weight of the sample, combined with the particle size data is used to calculate the aerosol particle concentration.

LIGHT FILTER

The yellow filters worn by the subjects were described in Section II and their optical properties illustrated in Figure 2. In the experiments, subjects who normally did not wear corrective glasses used spectacles fitted with the filter lenses without refractive correction. Subjects who normally wore corrective glasses were provided with clip-on filters.

EXPERIMENTAL PROCEDURE

In the tests, a Landolt C chart rested on a stand inclined at 45° to the horizontal, and directly below the light. The center of the chart was 9 ft below the light and faced the observer who was at the upper level shown in Figure 9,
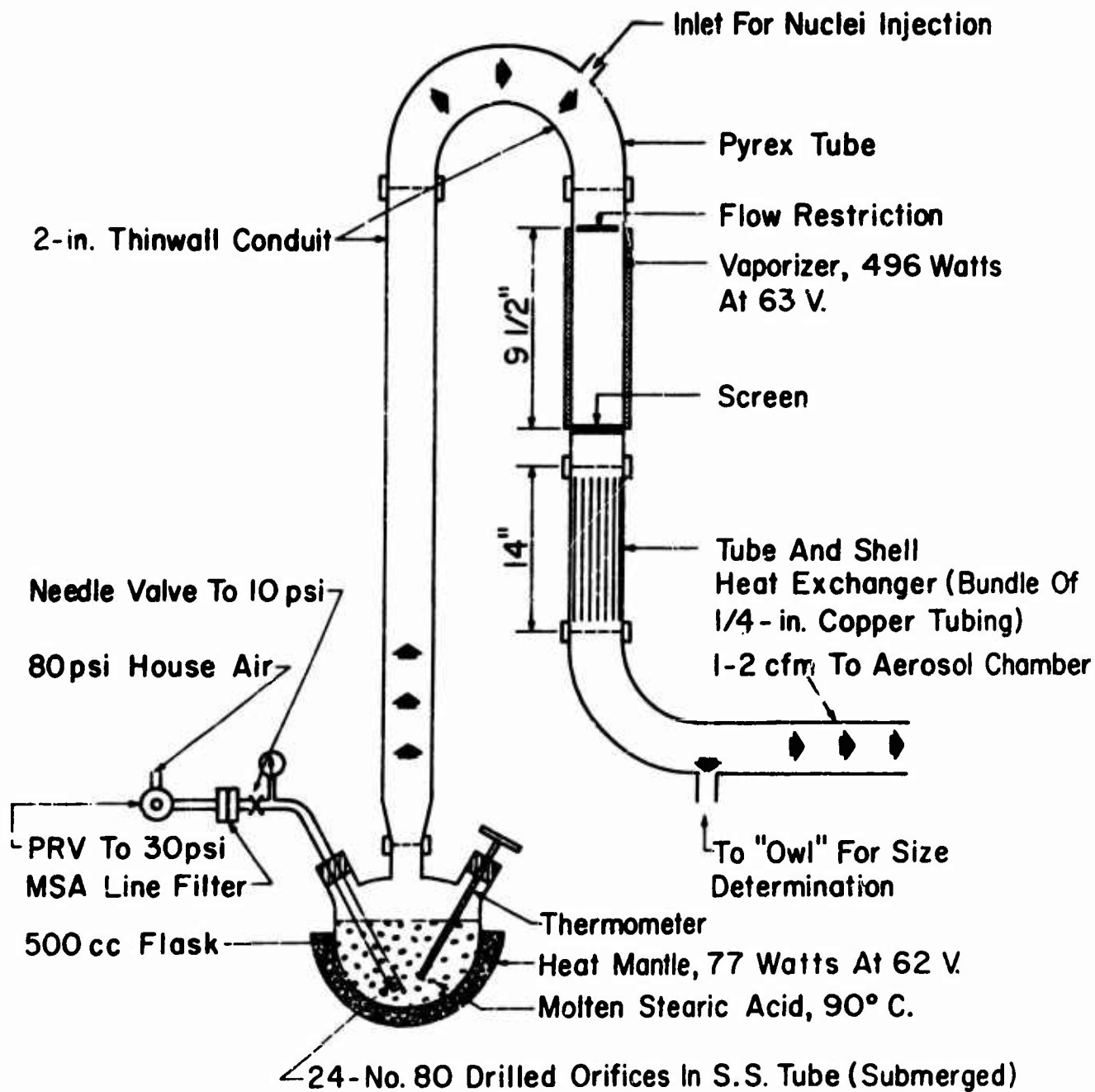
Figure 11. HIGH VOLUME MONODISPERSE STEARIC ACID AEROSOL GENERATOR
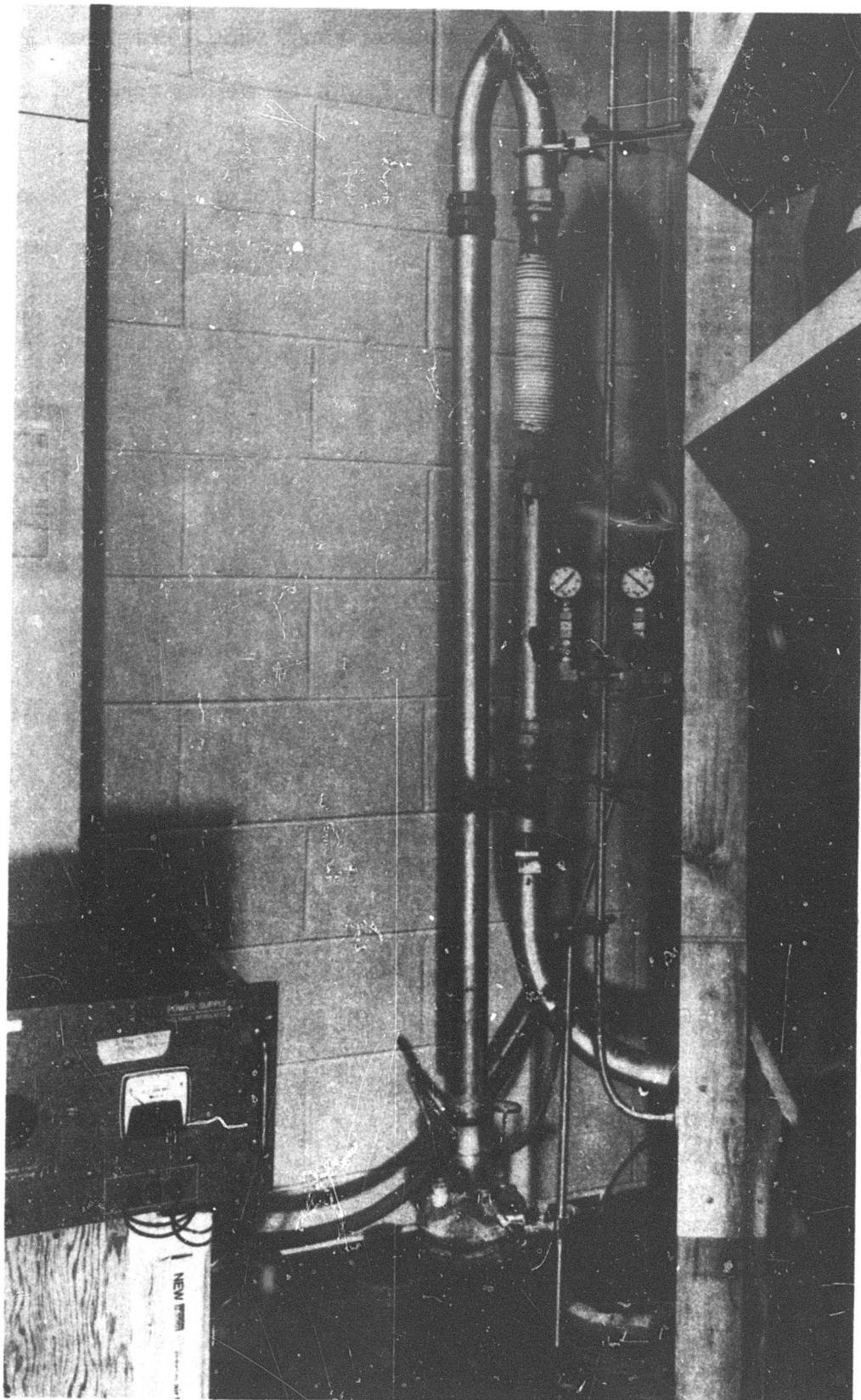
Figure 12. LaMer Generator

12.7 ft from the chart and 9 ft from the light. Figure 13 shows a view of the chart and the light as seen from the observer's gallery.

Each subject was given the sheet of instructions shown in Appendix IV. He was then dark adapted for 15 min in the test chamber. At the start of the test the flare simulation light was turned on and the subject moved to the test position, opened a window into the chamber, placed his chin on a rest, and read the chart to the experimenter by identifying the directions of the Landolt C's.

Readings were continued from large to small sizes until the subject could no longer distinguish the letters. The subjects used both eyes with no restrictions on head movement. Each subject was allowed as much time as he required which, in general, was no more than about 2 min on the most difficult lines. Each subject was urged to read beyond the point where complete certainty could be maintained. The readings were surprisingly accurate even when the subjects believed they were guessing. The subjects found it especially difficult to read when accuracy better than 80% could not be maintained.

Each subject performed four tests:

(1) Unfiltered vision at the low illumination level
(2) Filtered vision at the low illumination level
(3) Unfiltered vision at the high illumination level
(4) Filtered vision at the high illumination level.

36
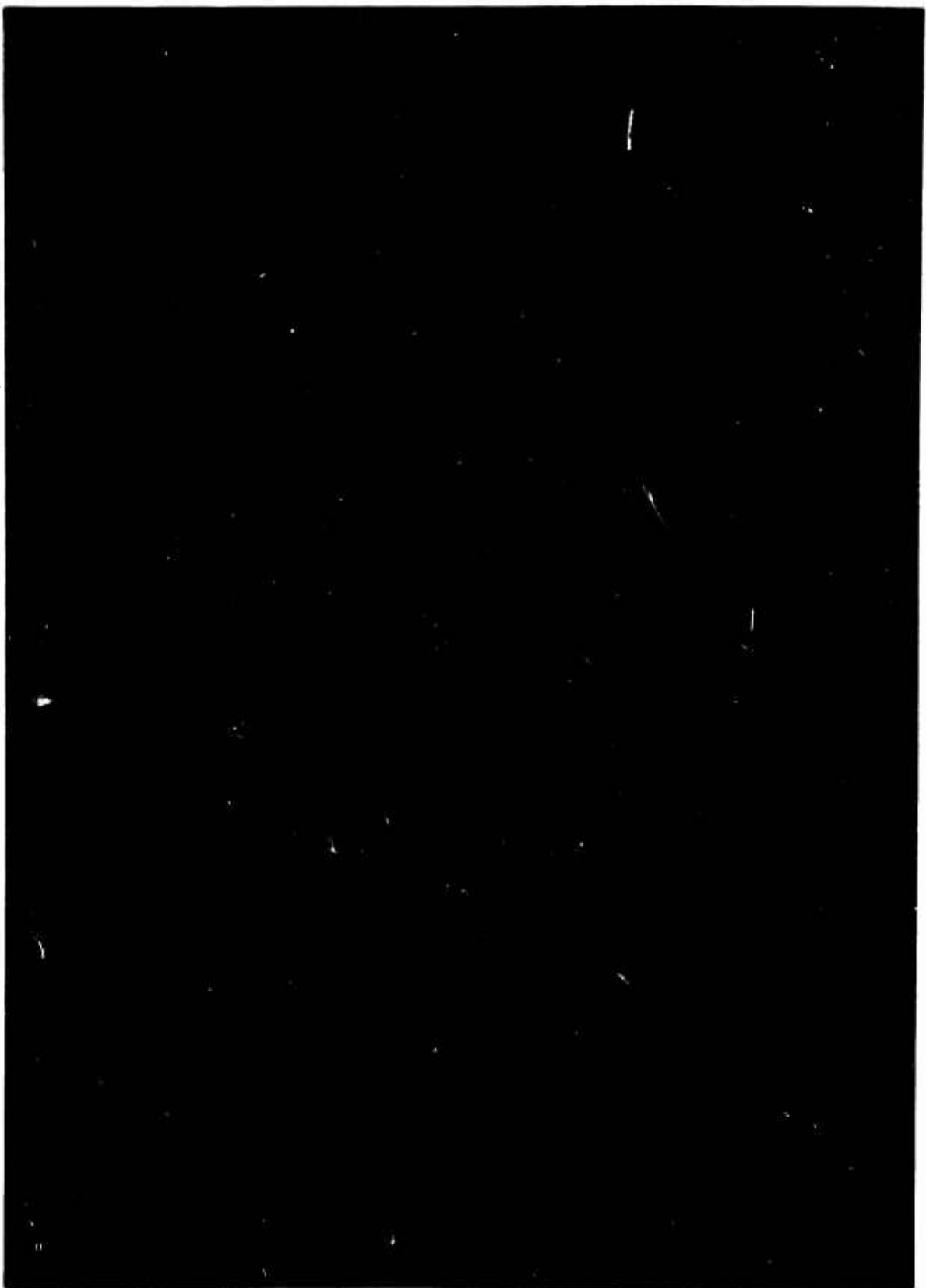
Figure 13.   TEST CHAMBER WITH LIGHT SOURCE AND
LANDOLT C CHART

The test sequence was random and charts were changed after each test. The chart size range permitted the subject to reach the center of the chart without too much difficulty but not to reach the end of the chart with any assurance of correctness. The chart range tended to minimize premature discouragement and to accommodate the maximum in visual performance.

The 30 subjects were divided into three groups of 10. One group was tested in the chamber without an aerosol, the second was tested with a light aerosol haze generated for 5 min, and the third group was tested with a denser, 10 min aerosol.

The aerosol size was measured (see Appendix III) at the start of each subject's test series and the aerosol concentration was determined by a filter sampling at three equally spaced intervals during the tests. Optical measurements indicated a particle diameter of 0.68 microns. Particle concentrations were 2.5×10^5 and 5.0×10^5 particles/ml for the 5 and 10 min aerosols, respectively. The linear relation between aerosol generation time and the aerosol concentration is evidence of the stability of both the aerosol generator and the aerosol itself.

A typical test sequence involving the pre-test dark adaption and four tests took about 45 min for each subject.

EXPERIMENT DESIGN

The experimental representation of the test is shown in Table 2. The experimental variables are

L_1 = 2,000,000 candlepower light source

L_2 = 5,000,000 candlepower light source

F_1 = no filter

F_2 = yellow filter

H_1 = no haze

H_2 = 5-min haze generation

H_3 = 10-min haze generation

R_1-R_{30} = experimental subject.

EXPERIMENTAL RESULTS

(1) DESCRIPTIVE RESULTS

The experimental results were tabulated as the total number of correct C's recorded for each subject in each test. Most subjects made a few errors before reaching their limits. In reporting the results it was decided to list the total number of correct readings, without weighting the errors. Since there were 70 different sizes of C's on each set of charts, each trial's result must be between 1 and 70. Thus 40 data points were obtained for each of the three groups of 10 subjects. The "raw" averaged data are shown in Table 3.

From these figures the corresponding size of Landolt C gap for each observation condition was computed (see Table 4). This is the visual angle of the smallest Landolt C gap

Table 2

Experimental design of the tests

First Set		Second Set		Third Set	
$L_1\ F_1\ H_1$		$L_1\ F_1\ H_2$		$L_1\ F_1\ H_3$	
$L_2\ F_1\ H_1$	R_1	$L_2\ F_1\ H_2$	R_{11}	$L_2\ F_1\ H_3$	R_{21}
$L_1\ F_2\ H_1$		$L_1\ F_2\ H_2$		$L_1\ F_2\ H_3$	
$L_2\ F_2\ H_1$		$L_2\ F_2\ H_2$		$L_2\ F_2\ H_3$	
"	R_2	"	R_{12}	"	R_{22}
"	R_3	"	R_{13}	"	R_{23}
"	R_4	"	R_{14}	"	R_{24}
"	R_5	"	R_{15}	"	R_{25}
"	R_6	"	R_{16}	"	R_{26}
"	R_7	"	R_{17}	"	R_{27}
"	R_8	"	R_{18}	"	R_{28}
"	R_9	"	R_{19}	"	R_{29}
"	R_{10}	"	R_{20}	"	R_{30}

correctly identified by the subjects. It is noted that the reciprocal of the Landolt C gap angle is sometimes termed the visual acuity. In the present report the term visual acuity is used in a more general, qualitative sense.

(2) QUALITATIVE DATA ANALYSIS

Simple inspection of the data shows clearly the qualitative relations of visual acuity with light intensity and fog density. Increased light intensity increases visual acuity while increased aerosol density decreases acuity.

There is no indication of improved visual response resulting from the use of the yellow filters; indeed the reverse is suggested by the data of Tables 3 and 4.

Table 3

Averaged numbers
of correct Landolt C readings

	$L_1 F_1$	$L_1 F_2$	$L_2 F_1$	$L_2 F_2$
H_1 (no haze)	54.8	54.6	57.2	55.0
H_2 (5 min haze)	49.4	48.1	51.9	52.1
H_3 (10 min haze)	44.2	42.4	48.6	48.3*

Table 4

Averages of correctly read
Landolt C gaps in minutes of arc
(visual angle)

	$L_1 F_1$	$L_1 F_2$	$L_2 F_1$	$L_2 F_2$
H_1 (no haze)	0.770	0.767	0.667	0.767
H_2 (5 min haze)	1.065	1.164	0.911	0.927
H_3 (10 min haze)	1.437	1.565	1.100	1.115

41

The statistical analyses of the data are discussed in the following section.

(3) STATISTICAL ANALYSIS OF THE EXPERIMENTAL DATA

The statistical examination of the data included an analysis of variance with tests of their statistical significance. Multiple regression equations were developed, specifying the functional relations between these performance measures and the controlled factors. A detailed description of the analysis is given in Appendix V, including a number of graphical presentations of the data.

The summarized data for the haze and light tests are given in Tables 5 and 6. In these tables, the observations with and without the filter are averaged.

Table 5

Mean number of symbols correctly identified
with various haze and light conditions

Light Intensity Symbol and Level (million CP)		Haze Level, Symbol and Generation Time, in minutes			
		H_1-0 min	H_2-5 min	H_3-10 min	Combined
L_1	2	54.80	48.75	42.80	48.78
L_2	5	56.10	52.10	48.45	52.22
Combined		55.45	50.42	45.62	50.50

42

Table 6

Mean values of smallest correctly identified
Landolt C visual angles in minutes of arc
with various haze and light conditions

Light Intensity Symbol and Level (million CP)		Haze Level, Symbol and Generation Time, in minutes			
		H_1-0 min	H_2-5 min	H_3-10 min	Combined
L_1	2	0.768	1.115	1.501	1.128
L_2	5	0.717	0.919	1.107	0.914
Combined		0.742	1.017	1.304	1.021

The tables emphasize the diminished visual efficiency caused by haze, and the improvement with increased light intensity. A uniform rate of visual degradation as the fog level increases occurs under both 2,000,000 and 5,000,000 candlepower light levels. The incremental degradation is about 6 units at the lower light level, and 4 at the higher.

The quantitative differences due to haze and to illumination level are statistically significant at the 0.001 probability level. The interaction data are significant at the 0.01 level or less. The data on the effect of the filter, which was noted as qualitatively unfavorable in the previous section, are not quite statistically significant at the 0.05 probability level.

Equations were developed, using the method of multiple regression, to correlate the visual response with the haze and illumination levels. When stated in terms of the number

43

of symbols, Y_1, correctly identified by a subject, the equation has the form

$$Y_1 = 50.500 - 4.921 \, X_1 + 1.717 \, X_3 + 1.088 \, X_1 \cdot X_3 \qquad (7)$$

In this equation, X_1 is the haze level and X_3 is the light level.* X_1 and X_3 are coded to facilitate the multiple regression analysis as follows.

Symbol	H_1	H_2	H_3
Haze level, min	0	5	10
Coded values, X_1 (linear scale)	-1	0	+1
Symbol	L_1	L_2	
Light level, million CP	2	5	
Coded values, X_3 (linear scale)	-1	1	

The product term, $X_1 \cdot X_3$ in Equation 7 is a consequence of the haze-light interaction.

---

*The symbols X_1 and X_3 are discussed in Appendix V.

SECTION IV

DISCUSSION

EXPERIMENTAL RESULTS

Some of the results appear obvious and predictable, but
some were unexpected. The decrease in visual acuity with
increased fog level was expected, and the increased acuity
with increased intensity of illumination was certainly not
surprising. The suggestion of a linear relation in the former
case was unexpected, as was the striking evidence of
interaction between haze level and light intensity.

The status of the yellow filter is not fully resolved. There
is however, clearly no evidence of its value as a visual aid
in a fog under the experimental conditions, i.e., the
observation of achromatic objects.

FACILITY

Within the limits of the present study the laboratory
facility has been found to be an efficient and reproducible
system. It would be desirable to characterize its performance
in an extended range of aerosols, including increased
concentrations and a number of aerosol particle sizes. High
concentrations and large particles may be expected to
diminish the stability of the aerosol and thus limit the
usefulness of the chamber. In addition it would be useful
to undertake direct experimental comparisons between the
environmental chamber and the real environment.

45

MISCELLANEOUS OBSERVATIONS

1. Test personnel tended to "feel" that they had reached their perceptual limit well before they actually had. A reluctance to fail appears to be involved; with some persuasion candidates usually succeeded in identifying additional letters beyond their point of first surrender.

2. A number of candidates felt more comfortable with the filter, although no measurable improvement was observed.

3. Few color deficient candidates were aware of their condition and they usually tended to disbelieve it, often with considerable emphasis.

SECTION V

RECOMMENDATIONS FOR FURTHER STUDIES

The availability of a laboratory facility for vision
studies in fogs and cloudy environments presents the opportunity
of studying a number of problems concerned with visual percep-
tion and relating them to practical situations. It is
recommended that these include

(A) The milkbowl effect. The effects of aerosol
concentrations, aerosol sizes, and light intensity should be
measured. The persistence of disorientation as a function
of these parameters should be determined. Theories of its
origin should be formulated and quantified and concentration
limits in the real environment should be determined. Means
of diminishing its adverse effects should be formulated.

(B) The observation noted in the present study that fog
density and light source brightness show an interaction in
their effect on the visual response requires further examina-
tion. The range of visual parameters should be enlarged. The
present results demonstrate the usefulness of the facility
well but cover a limited range of the conditions. The
observation of the decrease in the rate of change of visual
acuity with increased fog density as the source intensity
increases suggests that still larger flares would give better
vision control in foggy environments.

(C) The effect of haze under daylight conditions should
be studied. Color perception, including colored targets and

47

also colored light sources could easily be made a subject for examination in the present facility.

(D)   Studies should be made to correlate the effect of light scatter on vision. The contribution of scattered light to target illumination and background contrast require experimental verification of the theoretical analysis. The decrease of depth perception in fogs could be part of such an evaluation.

(E)   The filter observations should be extended to encompass both achromatic and chromatic conditions. Other filter concepts should be examined, based on existing theories of wavelength dependence of light scattering by small particles.

(F)   A wider range of fog densities should be explored, with ultimately consideration of laboratory simulation of the concentration levels associated with haze, mist, fog, clouds, rain, and snow.

(G)   Perception studies in the present report were made using a 45° angle between light, target, and subject. The effect of other viewing angles should be related to these results.

(H)   The use of other aerosol materials should be explored for more efficient and for a broader range of simulation of meteorological conditions.

APPENDIX I

LIGHT-SCATTERING FUNCTIONS

The light-scattering functions in Equation 4 contain the constants a_n and p_n, which are defined as follows:

$$a_r = \frac{\alpha P_n'(\beta)\ P_n(\alpha) - \beta P_n'(\alpha)\ P_n(\beta)}{\alpha P_n'(\beta)\ S_n(\alpha) - \beta S_n'(\alpha)\ P_n(\beta)}$$

and

$$P_n = \frac{\alpha P_n(\beta)\ P_n'(\alpha) - \beta P_n(\beta)\ P_n'(\beta)}{\alpha P_n(\beta)\ S_n'(\alpha) - \beta S_n(\alpha)\ P_n'(\beta)}$$

where

$\alpha = 2\pi r/\lambda$

$\beta = m\ \alpha$

m = the refractive index of the scatterer.

$$P_n(\alpha) = \left[\frac{\pi a}{2}\right]^{\frac{1}{2}} J_{n+\frac{1}{2}}(\alpha)$$

$$C_n(\alpha) = (-1)^n \left[\frac{\pi \alpha}{2}\right]^{\frac{1}{2}} J_{-n-\frac{1}{2}}(\alpha)$$

and

$$S_n(\alpha) = P_n(\alpha) + i\ C_n(\alpha)$$

The symbol $J_u(\alpha)$ represents a Bessel function of the order u, and the primes represent derivatives of the parent functions.

The coefficients of Equation 3, which describes the radial distribution of intensity of the scattered light are:

$$i_1(\theta) = \left[\sum_{n=1}^{\infty} \frac{2n+1}{n(n+1)} \left\{a_n\ S_n(v) + P_n\ t_n(v)\right\}\right]^2$$

49

$$i_2(\theta) = \left[\sum_{n=1}^{\infty} \frac{2n + 1}{n(n + 1)} \left\{ P_n S_n(v) + a_n t_n(v) \right\} \right]^2$$

$$S_n(v) = \frac{1}{\sin \theta} P_n^1(v)$$

and

$$t_n(v) = \frac{d}{d\theta} P_n^1(v)$$

$P_n^1(v)$ is the first associated Legendre function, and $v = \cos \theta$.

APPENDIX II

LANDOLT C CHART DESIGN

The test charts were designed as a variation of the standard
Landolt C visual acuity chart. In the standard chart, the C's
are arranged in sets of progressively decreasing size. In the
present system, the chart consists of 14 rows (sets) of 5 C's each,
with the C's diminishing geometrically in size. In addition,
closed circles of appropriate sizes are included in the charts.
In assembling the charts, the orientation of the C's was based
on a table of random numbers.

In constructing the chart, a size range,which bracketed the
most extreme conditions, was selected empirically. Thus, a C
with   outer diameter (OD) could be seen by the test observers
unde   :mum illumination and at maximum haze concentration
(Light I_-, Filter F_2, and Haze H_3). This size was selected for
the first letter of Set 1 of the chart. The first letters of
consecutive 5 element sets were 0.75 times the first letter of
the previous set. The final size, Set 14, was unresolvable under
the most favorable conditions. The sequence is shown in Table 7.
This table also gives the gap size of the corresponding C and the
gap angle measured at 12.7 ft, the distance to the observer.

51

Table 7
CONSTRUCTION OF THE LANDOLT C CHARTS

Set No.	C OD-cm	Gap Size, cm	Gap Angle, -min.	"Visual* Acuity"
1	10.00	2.00	17.7	0.056
2	7.50	1.50	13.3	0.075
3	5.62	1.12	10.0	0.1
4	4.21	0.843	7.5	0.13
5	3.16	0.632	5.6	0.18
6	2.37	0.474	4.2	0.24
7	1.78	0.356	3.2	0.31
8	1.33	0.267	2.4	0.42
9	1.00	0.200	1.4	0.71
10	0.75	0.150	1.3	0.77
11	0.562	0.112	1.0	1.0
12	0.421	0.0843	0.75	1.3
13	0.316	0.0632	0.56	1.8
14	0.237	0.0474	0.42	2.4
15	0.1778			

*Visual acuity is defined as the reciprocal of
the angle in minutes subtending a gap cor-
responding to the limit of perception. (See
Graham et al., Ref. 9, 1966, p. 324).

The full sequence is determined by noting that there are
70 letters in the complete set. The diameters form a geometric
progression, whose constant ratio is

$$\frac{D_{n+1}}{D_n}$$

52

where D_n and D_{n+1} are the diameters of two successive terms. Thus the rth term is equal to

$$D_o \left(\frac{D_{n+1}}{D_n} \right)^r$$

where D_o is the "zeroth" term.

Thus, for $r = 70$, $D_o = 10$, and $D_{70} = 0.1778$ (see Table 7).

$$D_r = D_o \left(\frac{D_{n+1}}{D_n} \right)^r$$

$$\frac{D_{n+1}}{D_n} = 0.9441$$

and

$$\frac{D_n}{D_{n+1}} = 1.0592$$

Then, 1.0592 is the factor relating two successive adjacent diameters in the 70-element chart.

53

APPENDIX III

HIGHER ORDER TYNDALL EFFECT

The principle of the application of the higher order
Tyndall effect is implicit in the radial distribution of scattering
intensity as illustrated in Figure 5. In an aerosol cloud, as
the angle of observation varies from 0 to 180° to the
incidental beam, using a white light source, a sequence of
spectral colors is observed. The color brightness is intensified
with the uniformity of particle size, and the number of times
the spectral sequence is repeated increases with droplet radius.
The red color in each sequence is the easiest to identify and the
usual method of measurement involves counting or observing the
red bands. Two general experimental methods are used. One may
observe the total number of red bands in a 180° arc, or one may
observe the angle at which the first red band appears. The
method used in the pres t study is the second one.

The instrument used is a modification of the "Owl" described
by Sinclair and illustrated in Figure 14. A sample of aerosol
is drawn into the cylindrical chamber and is illuminated by a
parallel beam of white light. Observation is made through a
telescope rotating about the central axis of the chamber. The
number of reds observed as a function of particle size is shown
for stearic acid in Figure 15.

Figure 15 includes a calculated curve which is applicable
for all refractive indices up to about 2.

The angular positions of the reds for stearic acid as a
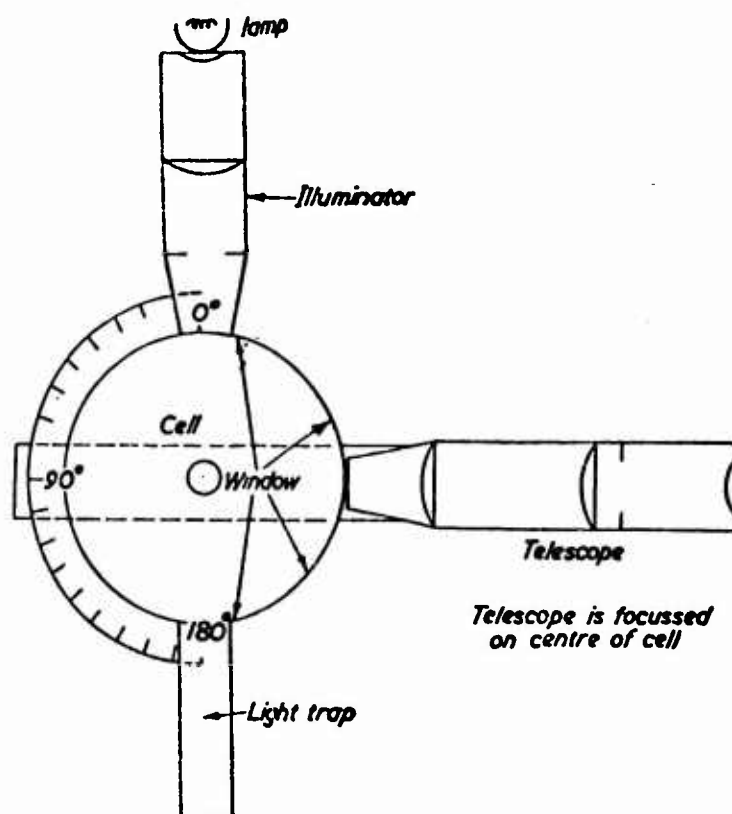
54

Figure 14. INSTRUMENT FOR MEASURING ANGULAR DISTRIBUTION
OF SPECIAL COLORS - THE OWL (SINCLAIR, 1950)
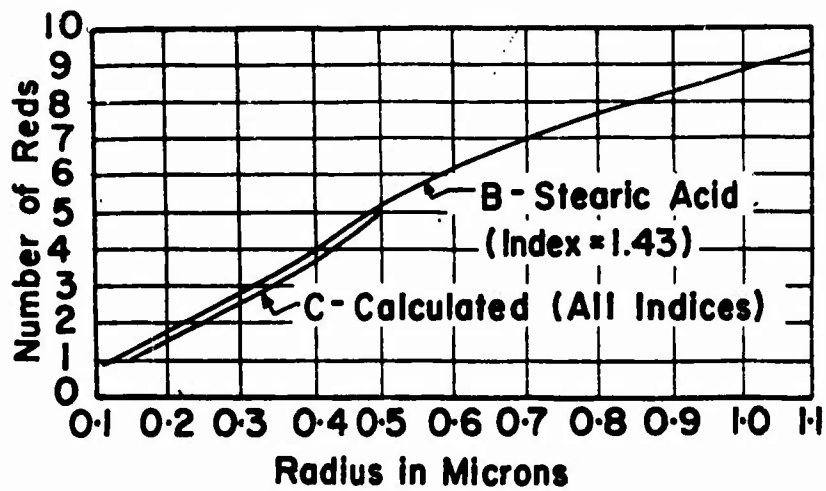
Figure 15.   OBSERVED AND THEORETICAL
            NUMBERS OF REDS PLOTTED
            AGAINST PARTICLE RADIUS
            (Sinclair 1950)
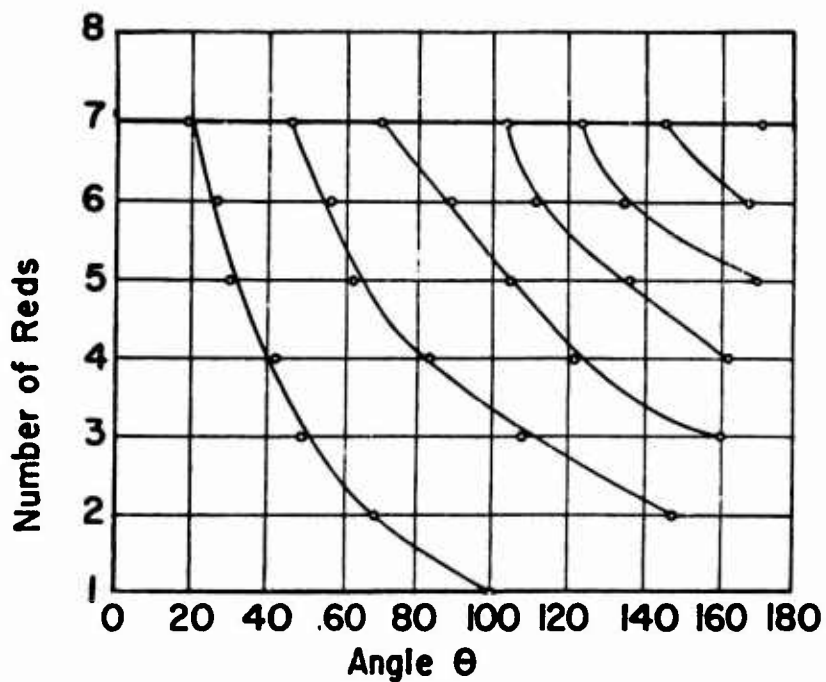
Figure 16. ANGULAR POSITION OF THE REDS
            FOR A STEARIC ACID AEROSOL
            (Sinclair and La Mer, 1949)

56

function of particle size is given in Figure 16 and the position of the first red band is shown in Figure 17. Figure 16 is based on an empirical relation between the angular position of the first red band, in degrees, and the mean radius in microns:

$$\log (\theta/10) + 1.43 \log (10r) = 1.43$$

This method is suitable for aerosol diameters between 0.4 and 1.5 microns.
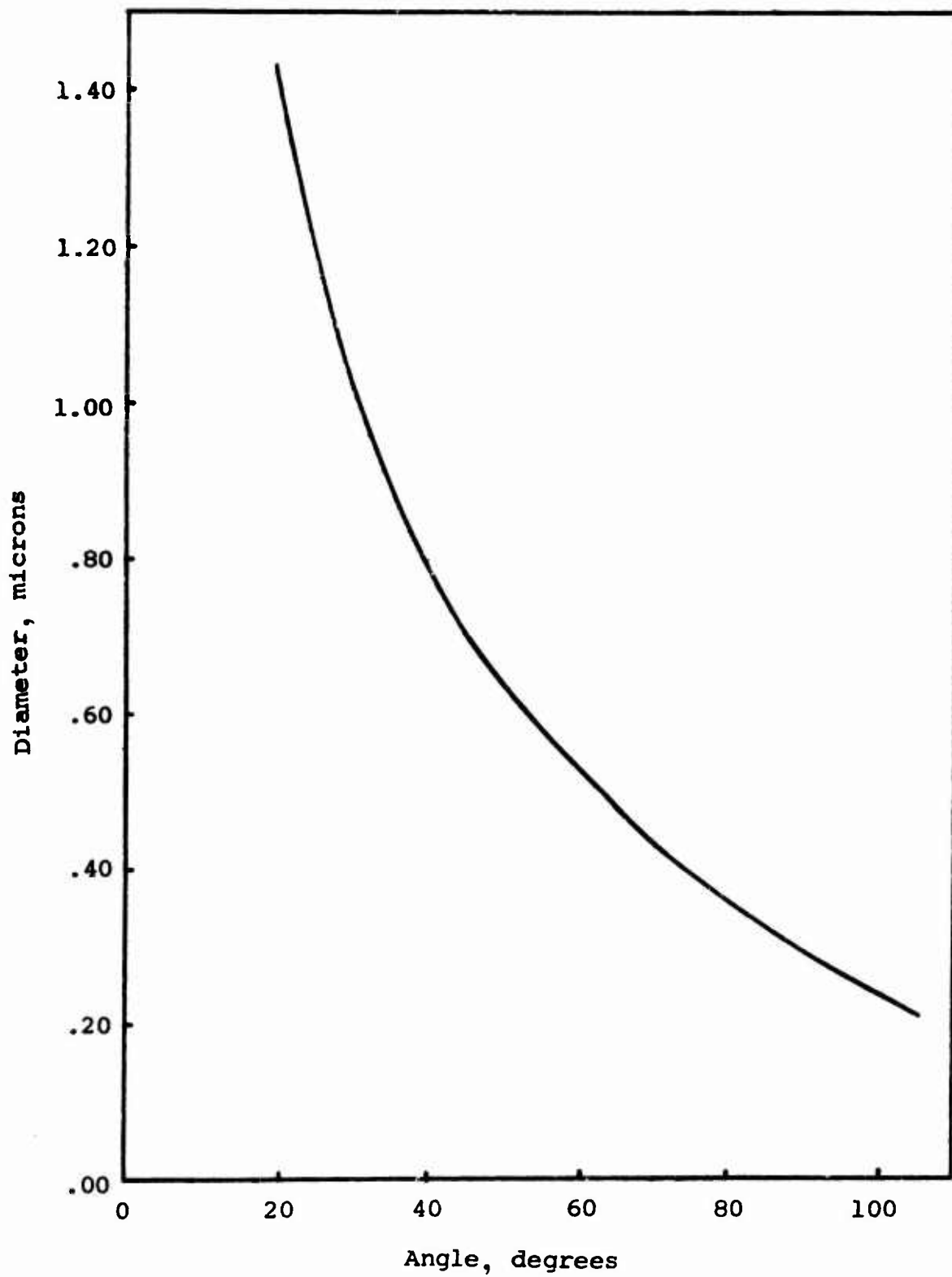
Figure 17. Angular Position of First Red Band
for Stearic Acid Aerosol (Sinclair
and LaMer, 1949).

APPENDIX IV

INSTRUCTION FOR THE SUBJECT

This is a visual perception experiment. We are asking
each of you (30) to help us measure your visual response under
a set of four (4) conditions at a given level of aerosol haze.
The four conditions consist of two light levels, with and
without a haze filter.

The initial dark adaptation will take 15 min. You may
drink coffee, but please do not smoke in the room. During the
test you will be standing on a scaffold and will be looking at
a chart at an angle of 45° below the horizon. The light source
will be at your eye level, directly over the chart. Please do
not attempt to shade the eyes to read the chart.

A chart of "c"s is used to measure your visual response.
The chart consists of the following figures:

| UP | DOWN | CIRCLE | RIGHT | LEFT |
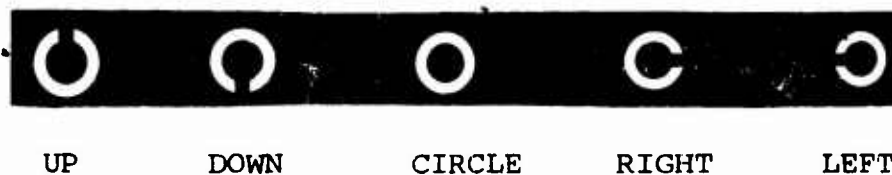
The names refer to the direction of the openings in the circles.
The figures are randomly arranged in rows of 5 each. The
figures are progressively smaller from left to right and from
top to bottom.

Using a row that is easy to read, start with the largest
letter (left) in the row. Describe the direction of the opening
as "left","right","up","down", or "circle". Read slowly enough
for the recorder to write down your answers.

59

It is most important to try to read as far down as you can. Many of the figures which you may think you are guessing are, in fact, correctly perceived. We don't want you to exhaust yourself in the process, but continue until you are sure you can not see the orientation of the figures any more.

RESULTS OF STATISTICAL ANALYSIS OF EXPERIMENT
ON FACTORS AFFECTING VISUAL ACUITY

PURPOSE AND SCOPE OF THE ANALYSIS

The data resulting from the psychometric experiment on
visual acuity that has been described in earlier sections of the
report were statistically analyzed to determine the effects of
the controlled factors on the performance of the subjects. An
analysis of variance with tests of statistical significance was
made on two different measures of visual acuity, and multiple
regression equations were developed specifying the functional
relationships between these performance measures and the
controlled factors. Diagrams are presented to show the nature
of the effects established by the analysis.

MEASURES OF VISUAL ACUITY (DEPENDENT VARIABLES)

The two measures of visual acuity subjected to statistical
analysis, designated Y_1 and Y_2, are as follows:

Y_1 Number of symbols of decreasing sizes correctly
identified by the subject.

Y_2 Visual acuity angle, i.e., the angle in minutes
subtended by the width of opening of a "C" of size Y_1.

CONTROLLED FACTORS (INDEPENDENT VARIABLES)

Three factors were systematically varied in the experiment
to determine their affects singly and jointly on visual acuity
as measured by the dependent variables. The target values or
levels of each of the three controlled factors are as follows,

61

expressed both in physical units and in corresponding coded values.

Haze Level

H, minutes of particle release	0	5	10
Coded values: X_1, linear effect	-1	0	1
X_2, quadratic	1	-2	1

Light Level

L, millions of candlepower (equivalent)	2	5
Coded values: X_3, linear effect	-1	1

Yellow Filter Glasses

F, whether glasses were used	No	Yes
Coded values: X_4, differential effect	-1	1

The coded values facilitate clearcut multiple regression analysis of the main effects and interactions of the independent variables through orthogonalization of the experiment design matrix.

Haze was present in the test chamber at three levels, with a group of ten subjects at each level. The three levels (the first of which is no release of particles) permit linear and quadratic (curvilinear) effects of haze level to be estimated in the regression analysis. Illumination was at two levels, permitting estimation of a linear effect of this variable. Filtering glasses were either worn or not; this is considered a discrete, two-valued variable that cannot take on intermediate values.

EXPERIMENTAL DESIGN

There were 30 subjects, assigned 10 to each haze level at random. Each subject was tested at the two light levels with and without the filtering glasses. Each of the 30 subjects was thus tested four times, giving a total of 120 chart readings and, finally, 120 values of Y_1 and Y_2.

The experiment design is a partially nested factorial, since a particular haze level applies to all four chart readings by any one subject whereas light and filter levels varied within subjects. The four possible combinations of the levels of these two factors define the conditions under which each subject read the charts.

The levels of the three controlled factors are the same throughout the experiment and are readily repeatable, hence the factors are treated as having "fixed effects." On the other hand, the 30 subjects are considered a random sample from an infinite population of persons meeting the selection criteria, hence differences among subjects are treated as "random effects."

This partially nested, partially crossed design with a mixture of fixed and random effects was specifically taken into account in carrying out the analysis of variance. An implication of this structure is that there are four different error terms for testing the statistical significance of the three independent variables and their interactions.

THE ANALYSES OF VARIANCE

Analyses of variance were made for both the number of symbols correctly identified (Y_1) and the visual acuity angle (Y_2). The

63

results are presented in Tables 8 and 9. A computer program, BMD-08V, written at UCLA was used for this purpose in conjunction with the IBM-360-50 computer at IITRI.

The values in the column headed "Probability, P" in the analysis-of-variance tables denote the range of probability P in which the magnitude of the effect associated with a particular identifiable source of variation might occur due, merely, to the residual variation or "error" inevitably present in the system. The insignificance of this random error increases the significance of the corresponding source of variation.

The same effects are significant in the two analyses: haze level, light level, and an interaction between the two. The haze and light effects are both highly significant; the evidence of an interaction between them is also very strong, particularly in terms of the acuity angle.

The mean values of a number of symbols correctly identified (Y_1), associated with the significant main effects and interaction, were given in Tables 5 and 6. Over the entire experiment the mean number correct was 50.50. As haze level increased from 0 to 5 to 10 min generation time the mean number of correctly identified symbols decreased from 55.45 to 50.42 to 45.62. Note that these values are very close to being equally spaced. As light level increased from 2 to 5 mcp the main effect was an increase in the mean number of correct identifications from 48.78 to 52.22. The nature of the significant interaction between haze and light levels is also apparent on examination of Table 5. One way of

64

Table 8

ANALYSIS OF VARIANCE FOR Y_1, NUMBER OF VISUAL SYMBOLS CORRECTLY IDENTIFIED

Source of Variation	Source Mean Square	Source Degrees of Freedom	Error Mean Square	Error Degrees of Freedom	Ratio of Mean Squares F	Probability P
MAIN EFFECTS						
H, Haze Level	965.474	2	42.187	27	22.88	<.001
L, Light Level	353.633	1	9.987	27	35.41	<.001
F, Filter or No Filter	17.633	1	5.875	27	3.00	.1
INTERACTIONS						
HL	47.355	2	9.987	27	4.74	.05>P>.01
HF	0.855	2	5.875	27	0.15	
LF	0.133	1	5.373	27	0.025	
HLF	8.407	2	5.373	27	1.56	>.2

Table 9

ANALYSIS OF VARIANCE FOR Y_2, VISUAL ACUITY ANGLE

Source of Variation	Source Mean Square	Source Degrees of Freedom	Error Mean Square	Error Degrees of Freedom	Ratio of Mean Squares F	Probability P
MAIN EFFECTS						
H, Haze Level	3.1553	2	0.1463	27	21.56	<.001
L, Light Level	1.3685	1	0.0352	27	38.90	<.001
F, Filter or No Filter	0.1045	1	0.0273	27	3.82	.1>P>.05
INTERACTIONS						
HL	0.2945	2	0.0352	27	8.37	.01>P>.001
HF	0.0014	2	0.0273	27	0.052	
LF	0.0072	1	0.0154	27	0.47	
HLF	0.0343	2	0.0154	27	2.23	.2>P>.1

stating this interaction is that the rate of degradation of performance with increasing haze is less at the higher light level than at the lower. There are about 6 units of difference between successive haze levels at the lower light level but only about 4 units of difference at the higher light level. The non-parallelism between the curves is shown graphically in Figure 18. The means are plotted as circled points. The 90% confidence limits (mean $\pm$ 1.2 units) are given by the vertical lines. The three means at each light level are connected by lines which separately bring out the approximately linear relationship between visual performance and haze level and in relationship to each other bring out the interaction between haze and light levels, i.e., the departure from parallelism.

The linear relations of Figure 18 between identified symbols and haze level are probably fortuitous. Visual angles are plotted against haze level in Figure 19, using the data in Table 10. The curves in the latter figure appear about as linear as the curves in Figure 18. The similarity in curvature of the two measures of visual acuity against the haze level indicate that, relative to each other, both measures would form a straight line over the same haze level interval.

The effect of wearing the glasses with filtering lenses is not quite significant at the 0.05 probability level (Table 3). The mean number of symbols correctly identified over the whole experiment with glasses worn was 50.12, compared with 50.88 without glasses. The difference is 0.77 units (mean score
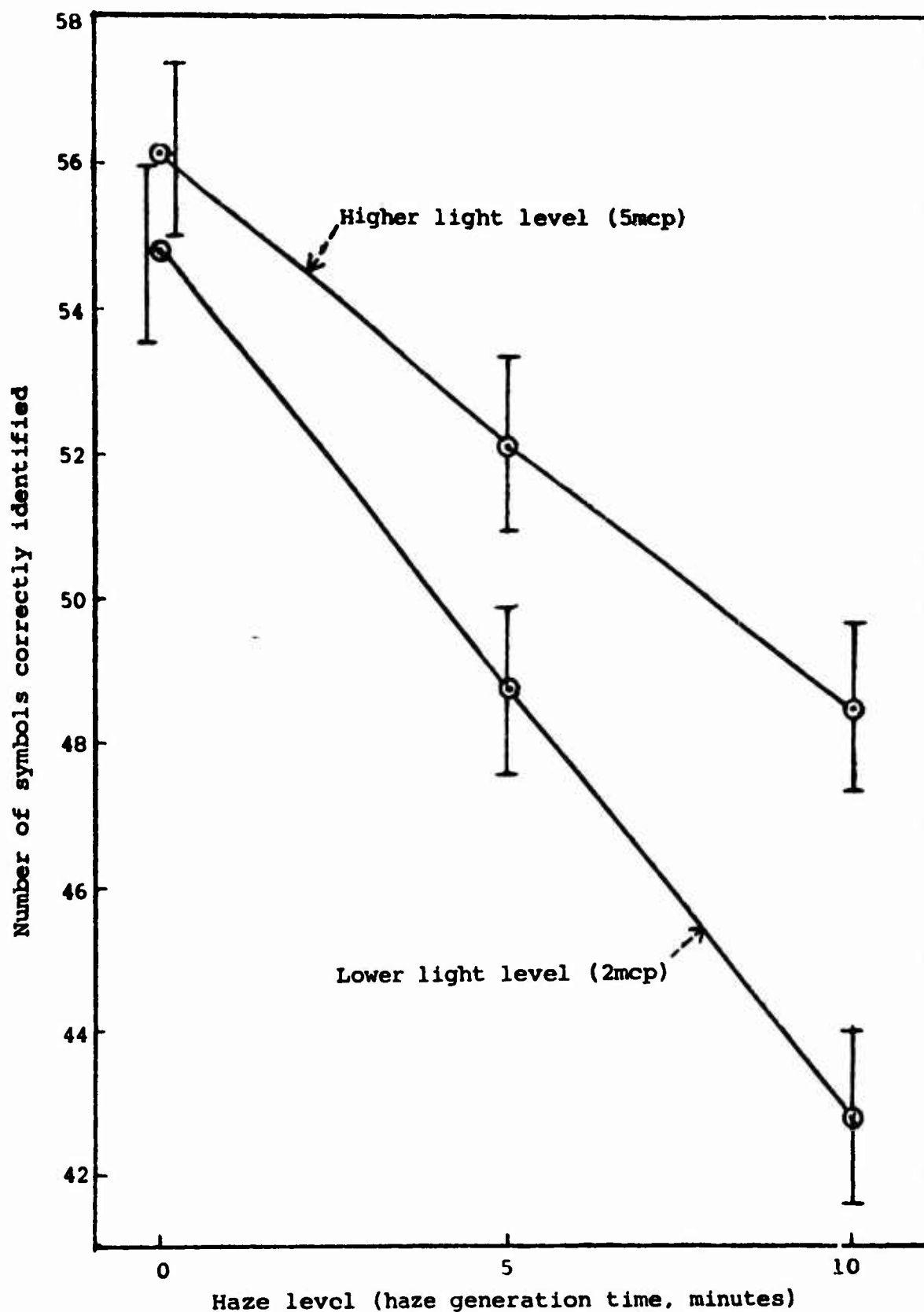
67

Figure 18. Mean values of Y_1 (number of symbols correctly identified), with 90% confidence limits, from experimental data on visual acuity at three haze levels under two levels of illumination.
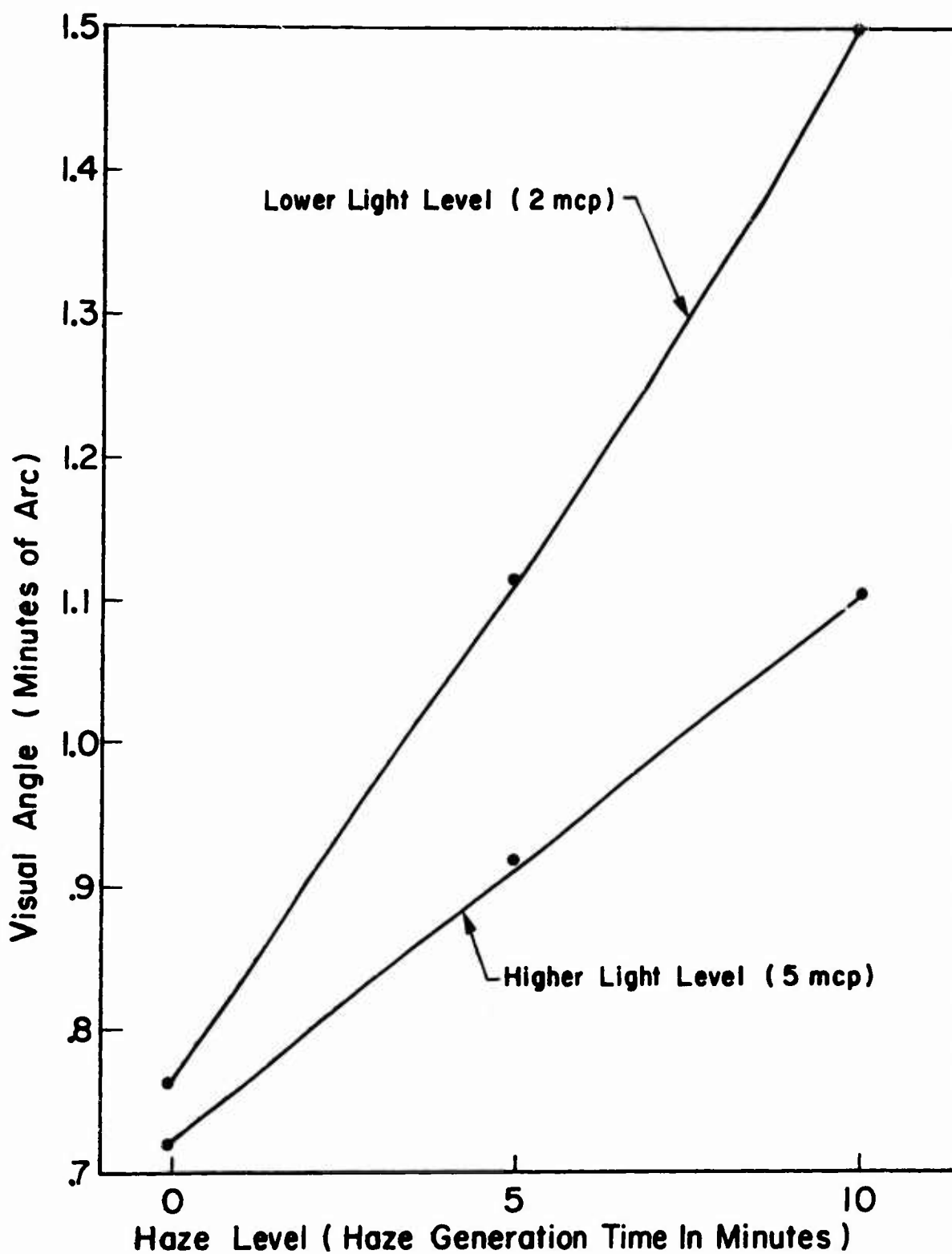
Figure 19.   MEAN VALUES OF VISUAL ANGLE AT THREE
HAZE LEVELS AND TWO LEVELS OF
ILLUMINATION

69

without glasses minus mean score with glasses). The 90%

confidence limits for this difference are 0.02 and 1.52 units.

The 95% confidence limits for the same difference are -0.14 units

and 1.68 units.

Table 6 gives the mean values for Y_2, the visual angle,

corresponding to the significant effects brought out in Table 8.

Y_1 and Y_2 are inversely related in the sense that values of Y_2

are large when values of Y_1 are small, and vice versa.

Otherwise, the interpretation of the results of the analysis of

variance in terms of Y_2 is similar to that already given in terms

of Y_1.

As measured by visual acuity angle the effect of the

filtering glasses is again not statistically significant at the

0.05 probability level (Table 8). The mean acuity angle over

the whole experiment with subjects wearing the glasses was 1.0506

and without the glasses was 0.9916 minutes. The difference is

0.0590 minutes (mean angle with glasses minus mean angle without).

The 90% confidence limits for this difference are 0.0076 and 0.1104

minutes of angle. The 95% confidence limits are -0.0030 and 0.1210

minutes of angle.

STATISTICAL RESPONSE EQUATIONS AND CONTOUR PLOTS

Statistical response (multiple regressions) equations were

fitted to the experimental data to provide a mathematical

description of the way the chosen dependent variables, Y_1 and

Y_2, are functionally related to the significant independent

variables, X_1 and X_3, over the field of joint variation of the

70

latter. A stepwise multiple regression program, 3MD-02R, written
at UCLA was utilized for this purpose in conjunction with the
IBM 360-50 computer at IITRI.

The resulting response equations are as follows:

$$Y_1 = 50.500 - 4.912X_1 + 1.717X_3 + 1.088X_1X_3$$

$$Y_2 = 1.0211 + 0.2808X_1 - 0.1068X_3 - 0.0855X_1X_3$$

These equations for Y_1 and Y_2 are expressed in terms of the
independent variables X_1 (coded haze level) and X_3 (coded light
level) and their multiplicative interaction. The form of these
equations is in agreement with the effects found to be significant
in the analyses of variance.

The following equations map physical values of haze intensity
and light intensity into the coded values as defined earlier.

$$X_1 = (H - 5)/5$$
$$X_2 = 3X_1^2 - 2$$
$$X_3 = (L - 3.5)/1.5$$

Filtering glasses can be either used or not, hence X_4 takes on
only the discrete coded values -1 and +1.

Contour diagrams constructed from the equations for Y_1 and
Y_2 are shown in Figures 20 and 21, respectively. These are
representations of the response surfaces, i.e., isocontour
curves of equal value of the dependent variable are arranged over
the field of joint variation of the two independent variables.
The net response (visual acuity as measured either by number of
symbols correctly identified or by acuity angle) at each point

71

Table 10

MEAN VISUAL ACUITY ANGLE (Y_2) UNDER TESTED COMBINATIONS OF HAZE AND LIGHT CONDITIONS

Light Intensity mcp	Haze Generation Time, Minutes			Combined
	0	5	10	
2	0.768	1.115	1.501	1.128
5	0.717	0.919	1.107	0.914
Combined	0.742	1.017	1.304	1.021

72

is the sum of the linear effects of haze and light level and their bilinear interaction. The way in which the mean response changes as haze level varies at any fixed light level, as light level varies at any fixed haze level, or as haze level and light level vary simultaneously, is clearly revealed by the diagrams.
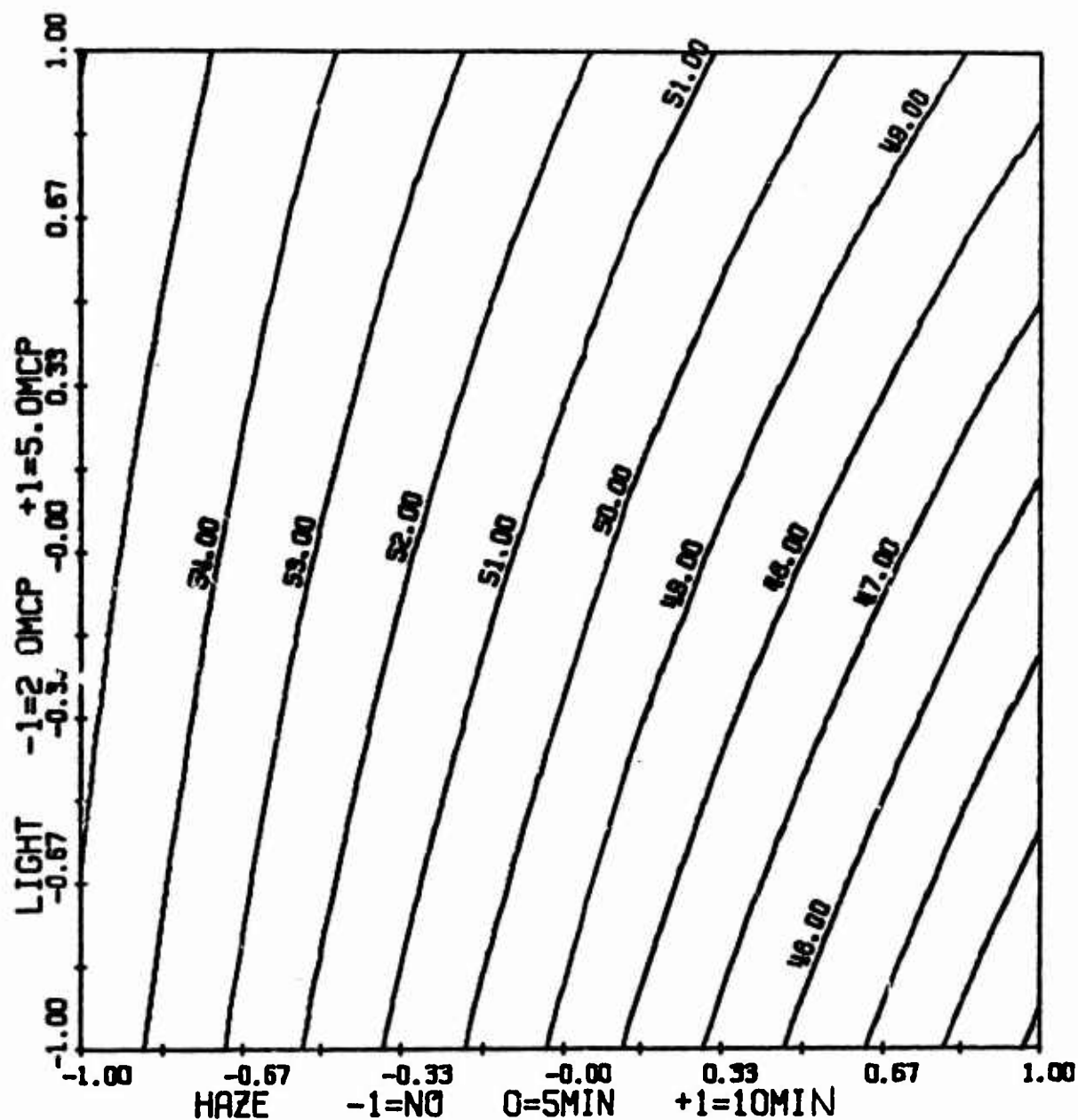
Figure 20. Isocontours of Y_1 (number of symbols correctly identified) over the field of joint variation of haze level and light level, computed from the response equation.
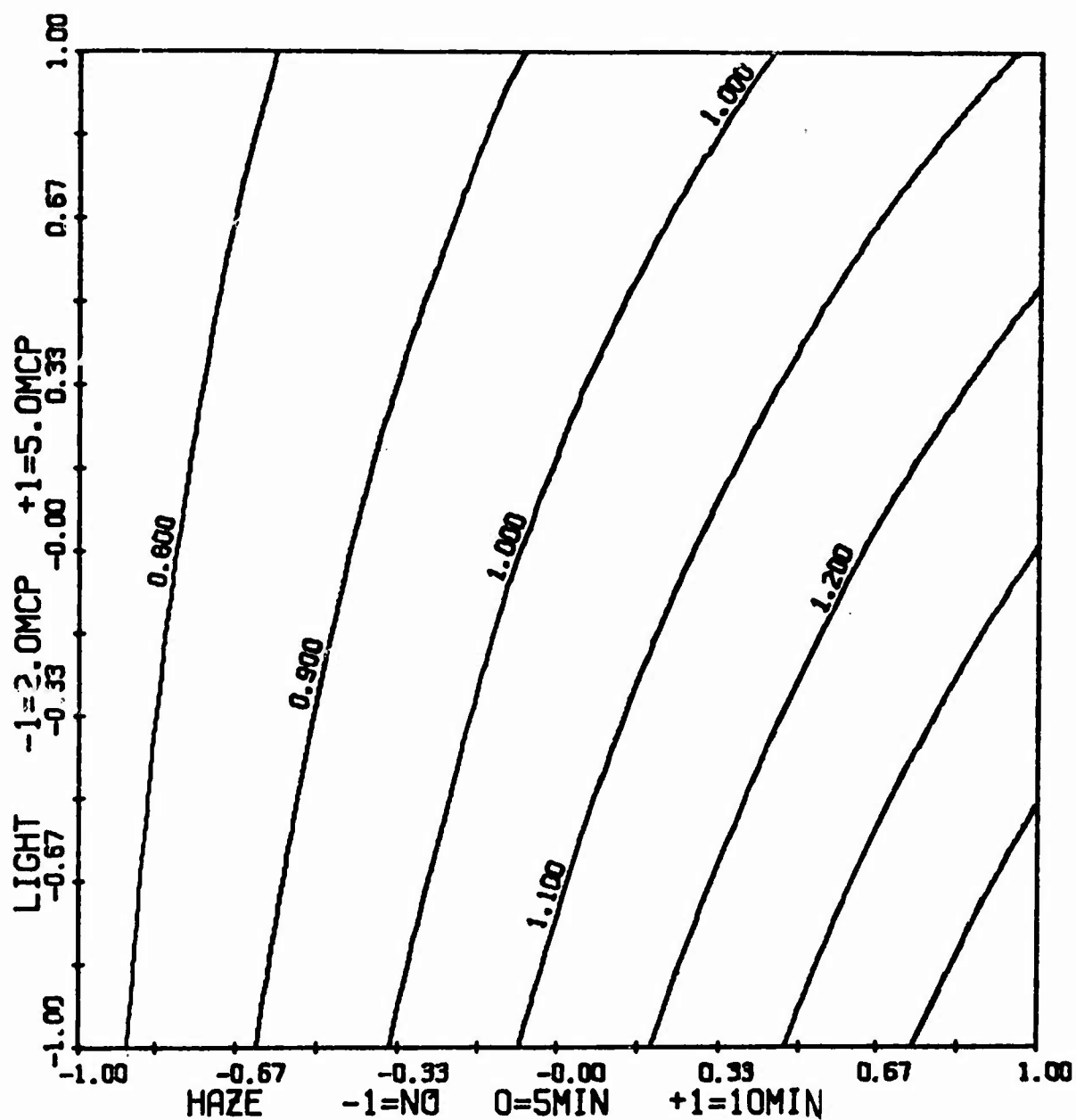
Figure 21. Isocontours of Y_2 (acuity angle) over the field of joint variation of haze level and light level, computed from the response equation.

REFERENCES

Brichard, J. La Meteorologie, 1939, 15, 83.

Blackwell, H.R., J. Opt. Soc. Am., 1946, 36, 624.

Graham, C.H., Bartlett, N.R., Brown, J.L., et al., Vision and Visual Perception, New York, Wiley, 1966.

Green, H.L. and Lane, W.R., Particle Clouds, London, 1964.

Hilgendorf, R.L., Visual Search and Detection under Simulated Flare Light, AMRL-TR-68-112, Aerospace Medical Research Laboratories, Wright-Patterson Air Force Base, Ohio, August, 1968.

Houghton, H.G., J. Aer. Sci., 1939, 9, 103.

Houghton, H.G., and Radford, W.H., Physics, Oceanography and Meteorology, 6, No. 4, Cambridge, Mass., 1938.

Kitani, S., J. Coll. Sci., 1960, 15, 287.

Kneusel, S., Meteorolog. Zeits. 1935, 52, 64.

Middleton, W.E.K., Vision through the Atmosphere, Toronto, University of Toronto Press, 1952.

Mie, G., Ann Physik, 1908, 25, 377.

Miller, J.S., Martin, B.C., and Dohrn, R.D. The Use of Yellow Lenses in Air Force Operations, SAM-TR-68-93, School of Aerospace Medicine, Brooks Air Force Base, 1968.

Rayleigh, Lord, Scientific Papers, Vol. 1 and 4, London, Cambridge University Press, 1899.

Sawyer, K.F., Thorpe's Dictionary of Applied Chemistry, 4th Edition, Vol. 10, London, Longmans, Green, 1950.

Sinclair, D., Handbook on Aerosols, Chapter 7, Washington, U.S. Atomic Energy Commission, 1950.

Sinclair, D. and La Mer, V.K., Chem. Rev., 1949, 44, 245.

Stuart, A.H., Engineering, 1934, 138, 107.

DOCUMENT CONTROL DATA - R & D

Security classification of title, body of abstract and indexing annotation must be entered when the overall report is classified

1. ORIGINATING ACTIVITY (Corporate author)		2a. REPORT SECURITY CLASSIFICATION
IIT Research Institute Aerospace Medical &		Unclassified
10 West 35th Street Research Lab., *AMD,		2b. GROUP
Chicago, Illinois 60616 AFSC, W-PAFB, OH 45433		N/A

3. REPORT TITLE

Visual Performance with Simulated Flarelight in Experimental Clouds.

4. DESCRIPTIVE NOTES (Type of report and inclusive dates)

Final Report, February 1969 - August 1969

5. AUTHOR(S) (First name, middle initial, last name)

Sidney Katz*   Elliot Raisen*

Paul K. Ase*   Robert L. Hilgendorf**

6. REPORT DATE	7a. TOTAL NO. OF PAGES	7b. NO. OF REFS
January 1970	76	17

8a. CONTRACT OR GRANT NO. In part under	9a. ORIGINATOR'S REPORT NUMBER(S)
F 33615-69-C-1386	C6173-1
b. PROJECT NO. 7184	
c. Task No. 05	9b. OTHER REPORT NO(S) (Any other numbers that may be assigned this report)
d. Work Unit No. 020	AMRL-TR-69-121 AD 704 125

10. DISTRIBUTION STATEMENT

This document has been approved for public release and sale; its distribution is unlimited.

11. SUPPLEMENTARY NOTES	12. SPONSORING MILITARY ACTIVITY
	Aerospace Medical Research Lab.
	Aerospace Medical Div., Air Force
	Systems Command, Wright-Pat. AFB, OH

13. ABSTRACT

An environmental chamber was designed for the study of visual acuity in simulated fogs and mists. Light scattering theory was used as a basis for the design of aerosol clouds with visual attenuation comparable with that of real fogs. An experimental generator was constructed to produce the aerosols.

A study was made of the visual responses of thirty subjects under simulated night conditions with flare illumination. The variables studied included fog density, flare intensity, and a comparison between unfiltered vision and vision through a yellow haze filter. A direct correlation was observed between visual acuity and fog density levels. An interaction was also noted between visual acuity, fog concentration, and light level within the ranges studied. At increased light levels, subjects tended to show slightly less sensitivity to changes in the fog density. No evidence of improved visual performance was observed when the yellow haze filter was used.

Key Words: Vision, Visibility, Perception, Field Illumination, Illuminating
             Flares, Reduced Visibility, Haze, Mist, Fog, Artificial Clouds,
             Simulation, Visual Performance, Haze Filter

DD FORM NOV 65 1473